University of Stavanger

Faculty of Science and Technology

MASTER'S THESIS

Study program/ Specialization: Offshore Technology – Industrial Asset Management	Spring semester, 2014 Open
Writer: Erik Kim Sandved	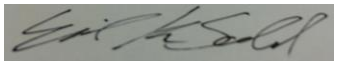 …… (Writer's signature)
Faculty supervisor: External supervisor: R.M. Chandima Ratnayake	
Thesis title: Using Numerical Analysis Tools to Increase the Reliability of Ultrasonic None Intrusive Inspection Results for In-service Pipeline Flanges	
Credits (ECTS): 30	
Key words: Ultrasonic inspection None destructive examination Finite element analysis	Pages: 19 + enclosure: 28 Stavanger, 10.06.2014 Date/year

Table of Contents

1. Abbreviations and terms

The following are a list of abbreviations and/or terms that are used in this report.

NCS: Norwegian Continental Shelf

RF: Raised Face

RFF: Raised Face Flange

RTJ: Ring Type Joint

RTJF: Ring Type Joint Flange

PA: Phased Array

FE: Finite Element

FEM: Finite Element Method

FEA: Finite Element Analysis

NDE: None Destructive Examination [1]

NDT: None Destructive Testing

NDI: None Destructive Inspection

NII: None Intrusive Inspection

UT: Ultrasonic Transducer

UTP: Ultrasonic Transducer Probe

HAZ: Heat Affected Zone

[1] NDE, NDI, NDT, and NII commonly interchangeable terms

2. Choice of topic and acknowledgements

At the start of my professional career I was involved in stress analysis of steel frame structures. Often, indeterminate structural systems were simulated with modern FEA software tools. At a later stage in my career I got involved with inspection and maintenance of offshore platforms, with a leading NCS engineering service provider. I was involved with in-service inspection services for topside static assets. Not long after working in the inspection group I noticed the limitations of UT inspection on certain in-service components. I became curious to see what had been done within the wider UT inspection community with respect to utilizing FEA simulations. There did not seem to be any particular reason that ultrasonic waves in metallic objects could not be modeled in a simulation tool. If these capabilities were packaged in a user friendly software suit, then the application of simulation techniques might help solve some of the problems previously experience when applying UT ultrasonics to in-service complex components.

I would like to thank my professors at UiS for their tutelage and patience. In particular, I would like to thank Professor R.M. Chandima Ratnayake who patiently listened and guided my ambitions. I would also like to thank Jan Dybdal and Trond Nordvik from Aker Solutions MMO who took time and interest at the expense of a busy schedules. Without their technical guidance this endeavor would most likely turned out quite differently. Finally, I would like to thank my family and friends that I could count on, for support, when the going got tough.

3. Introduction

3.1. Problem description

Ensuring the containment functionality of offshore topsides static assets such as pipes, valve bodies, pressure vessels, and storage tanks is vital in ensuring technical safety, reducing environmental impacts, and maintaining production up-times. Often, NDE methods are utilized to monitor the condition of in-service assets in order to control containment functionality. Different NDE methods are utilized for different applications. Each method has its benefits and limitations. For example, ultrasonic wall thickness measurements are common in identifying erosion and corrosion degradation of pipe spools with wall thickness above ~5mm, see figure 2-1.

Ultrasonic NDE techniques are commonly used to monitor material degradation of in-service components such as pipe spools and welded pipe joints. As the component geometries of pipe spools and welds are simple, determining the material losses over time is a matter of measuring the wall thickness of the pipe, similar to measuring the thickness of a plate of steel with a UT probe. Measuring the time delay, from initial transducer signal release until back wall reflected signal is received, by the transducer is an effective way of monitoring material losses over time. For components with simple cross-sectional geometry the back wall echo signal, received by the transducer, can easily be interpreted by a trained inspector.

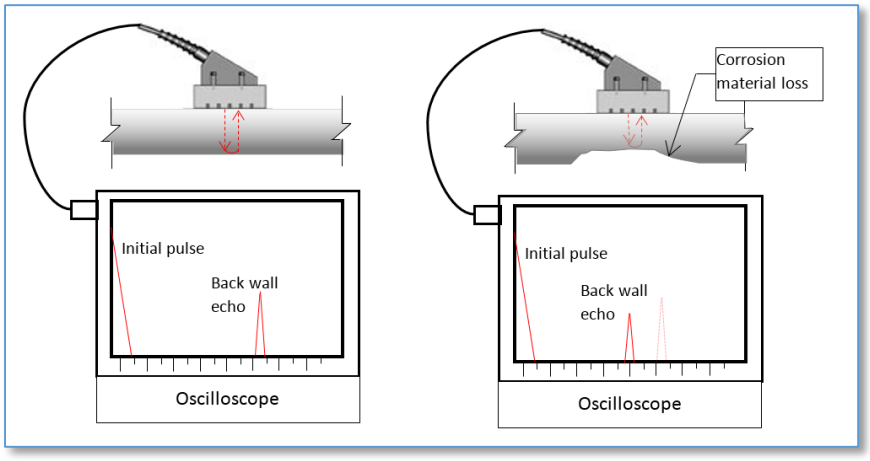

Figure 2-1: Material loss detection with 0 deg. UT probes. Note the relatively simple signal read outs on the oscilloscope. Each signal is intuitively linked to the beams flight of path.

Certain components such as pipe flanges, tank nozzles, and weldolets are challenging to inspect with ultrasonic NDE due to complex signal interactions with component geometries and other phenomena that occur during interactions with defects. Even predicting the ultrasonic beam's flight of bath could prove to be challenging. In order for a trained inspector to fully understand the complex signals that occur given complex specimen geometries, it is typical to create mockup calibration blocks that represent the item of interest, see figure 2-2. The signals observed on calibration mockups are used as a bench mark to compare inspection result signals against. Creating several mockups is time consuming, technically challenging, and costly. Some of the technical challenges in creating mockups are accounting for specific internal material defects such as voids, cracks, and lack of fusion with respect to welded joints. Limitations of mockups will be further explored in following sections.

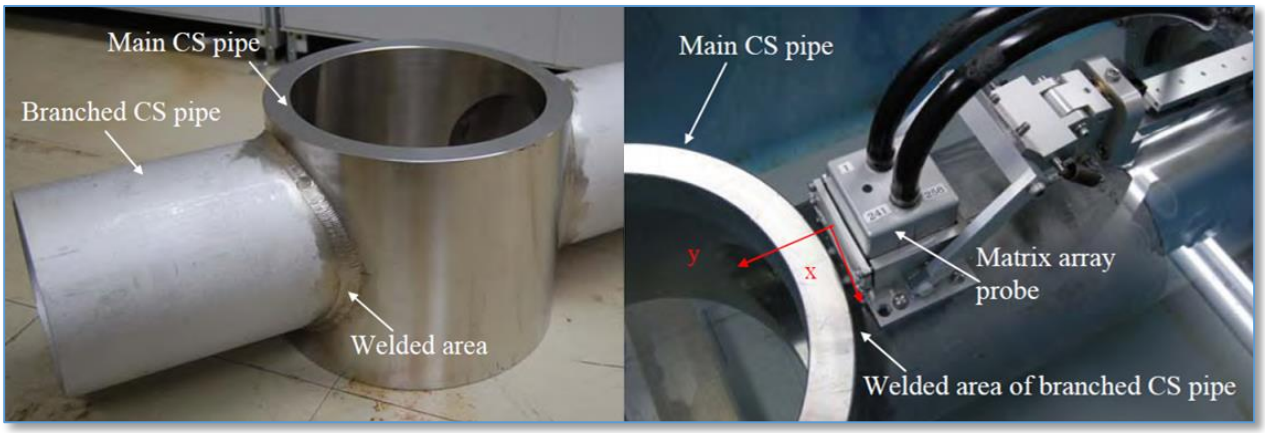

Figure 2-2: Mockups are commonly used to get a baseline UT signal that can be compared against when inspecting the actual component of interest. Note that several mockups, each with a different flaw, might be required if one is trying to identify the nature of a flaw in a component of interest.

In summary, the in-service ultrasonic inspection capabilities is limited to cases where the ultrasonic signals that are detected can be easily interpriated. Interpretation of the signals can be

relativly simple for a trained inspector as long as the component geometries are simple. Several components on an offshore production platform such as flanges, weldolets, and tank nozzles must be inspected visually during a shutdown since they are not always suited for other NDE techniques such as radiography and their complex geomoetries make ultrasonic inspection challenging. The signals that one will get during an ultrasonic inspection are too complex to interperate and mockups are impractical. Since most components are designed with a certain corrosion allowance it is not enough to simply conclude that a component is not fit for service if the inspection results for the component of interest is different from that observed on a zero flaw mockup. This paper will propose the utilization of modern FEA tools that will allow for simulations of ultrasonic testing on complex components and their constituent flaws in order to avoid the need to make multiple mockups. Simulated UT signal refference charts can be created for a wide selection of components. A wide array of flaws could also be accounted for via simulations, assuming siluations softare allows for accurate and diverse flaw modeling. The refference library will allow trained ultrasonic NDE inspectors to compare their inspection results against. If a match is found then there might be a reasonably high probability that the conditon of the in-service component matches that of the simulated case. This will further increasing the utility of ultrasonic NDE with respect to condition monitoring of in-service static assets on a typical offshore production platform.

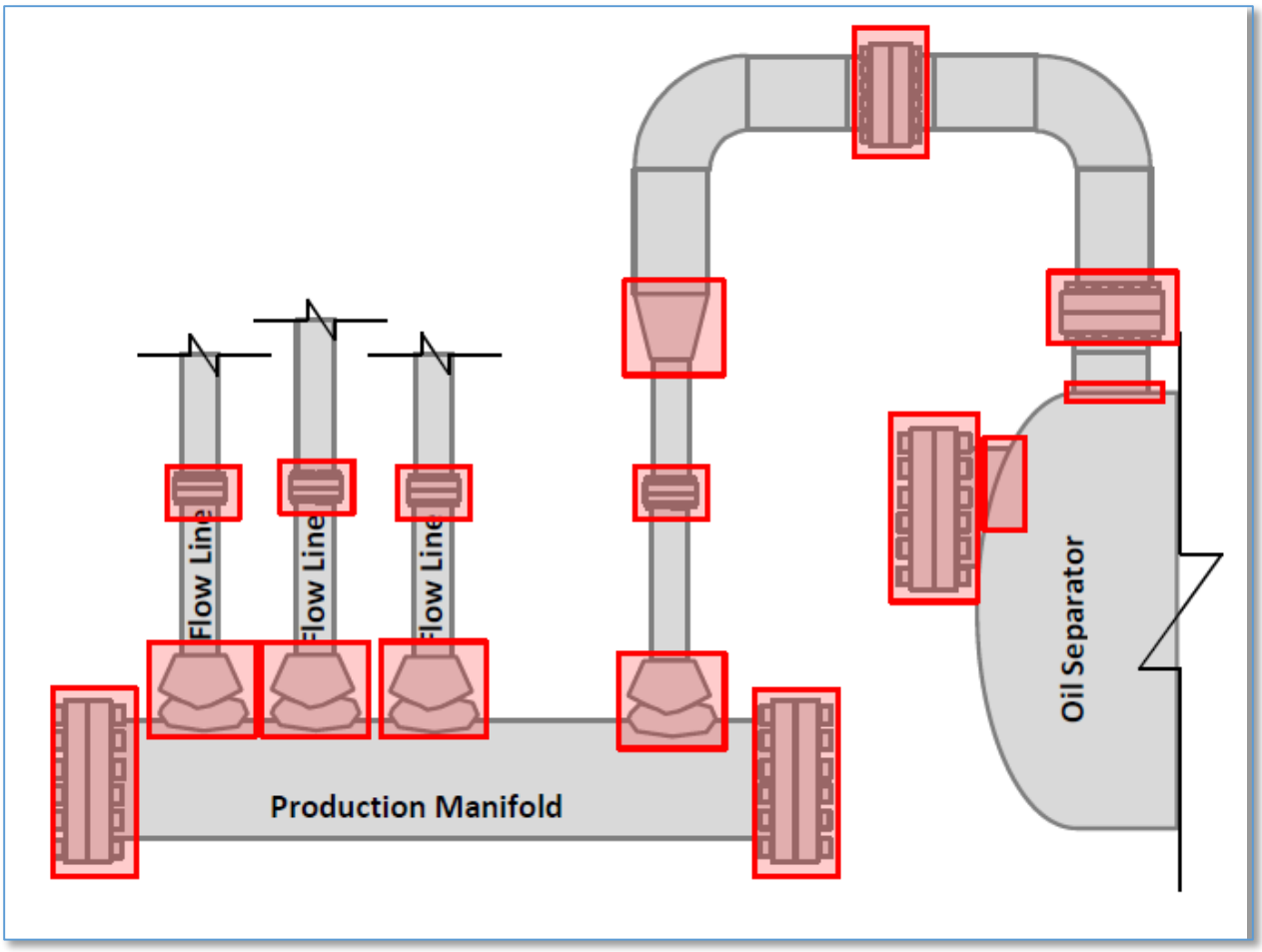

Figure 2-3: A rough schematic of oil producing flow lines, into a production manifold, before going into an oil seperator. Red boxes indicate areas where traditional NDE methods have proven challenging and often insuficient for reliable condition monitoring while assets are in-service.

As figure 2-3 indicate there are several locations that have a containment function such as pipe flanges, weldolets, reducers, T-joints, and tank nozzles. Several pipe flanges are considered critical with severar containment failure consequences.

3.2. Flange inspection case study

In this paper a specific case study on the implementation of ultrasonic NDE on flanges will be looked at in detail. Although the proposed implementation of simulation, utilizing numerical methods, can be practical for several scenarios, this paper will discuss the added benefits specifically to flange inspections. The flange problem also serves well as a technology and methodology test bed. Since the flange scenario covers all major aspects that are challenging to overcome without utilizing numerical methods such as complex geometries, placement of UT probe, and variability of degradation.

Flanged connections are commonly in use on pipelines with varying functions and mediums that they contain and transport, see figure 2-3. On an offshore production platform it is common to see flanged connections on lines that contain freshwater, sea water, air, stable and mixed unstable hydrocarbons in multiple phases. The most reliable method of verifying the containment functionality of a flanged connection is to visually inspect the contact surface between the flange face and its gasket. Visually inspecting the flange surface requires that the line is taken out of service. Given that several lines cannot be bypassed without total production shutdown, visual inspection of flanges are typically reserved for platform shut downs. It is of key financial interest to minimize shut down durations in order to reduce production down time and increase production up-time. Henceforth, limiting the required inspection scope during shutdowns has a direct and measurable economic benefit.

In order to help reduce the scope of visual inspection of flanges inspection service providers for the NCS have utilized phased array ultrasonic inspection technology. HOIS[2] Recommended Practice for in-service inspection of RF flange faces using phased array ultrasonic techniques outlines a variety of techniques that have been utilized and improved on by inspection service providers.

Although there are significant advantages of using phased array ultrasonic with respect to in-service inspection of flanges there are significant challenges to performing the inspection to ensure reliable results. There are multiple regions that the UT probe can be placed to run a scan. The most common practice to date has been placing the UT probe on the taper or just before the taper of the flange, see figure 2-4. Adjusting the angle of the ultrasonic beam to correctly target the region of interest on the flange seal area is critical (BURCH and COLLETT, 2012). Experience has shown that small variations in probe placement can affect the ability to

[2] Serving as a prime industry forum for inspection issues and improvements in inspection technology utilization, HOIS publishes a number of Recommended Practices. HOIS is managed by ESR Technology, a UK based engineering safety and risk consultancy.

accurately interpret the complex signals that result from these inspections. A UT probe rig has been designed and utilized to reduce the variability of probe placement. Once probe placement variability is minimized there are other aspects of the inherent geometry of the flange that still pose significant challenges to overcome. Manufacturing tolerances on certain areas of the flange are stringent and low enough to not affect the variability of inspection results. These regions are usually the machined flange surfaces. The manufacturing tolerances on other regions such as the taper are less stringent and at times can vary enough to affect the actual flight of path for the ultrasonic beam from the UT probe. The effect might be large enough to affect inspection results. Also, the surface finish on the taper can vary from very smooth to rough. The presence of surface coatings pose further challenges.

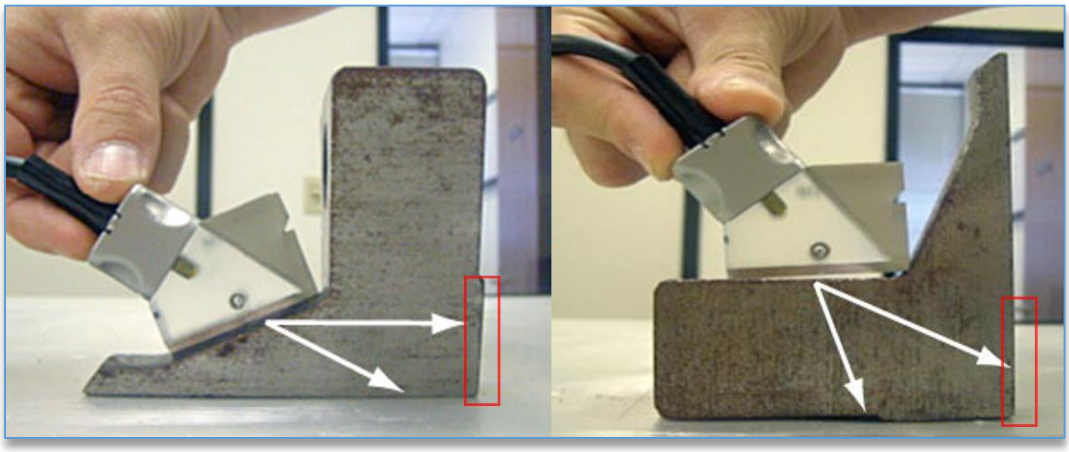

Figure 2-4: On the left a UT probe is placed on the flange taper versus the UT probe placed just before the taper as seen on the right image. Arrows show the path that ultrasonic waves will traverse, also referred to as the flight path. Region inside the red boxes are of primary interest as this is the sealing surface in contact with a gasket maintaining safe product containment.

3.3. Applicability of simulation tools

As indicated earlier mockups can be created to assist in deciphering ultrasonic inspection results. When performing an ultrasonic inspection on an object it is important to associate the signals displayed on the oscilloscope with the ultrasonic signals flight path. If the flight path of the ultrasonic beam gets scattered due to defects and or specimen geometry it is often challenging to interoperate results. When manufacturing metal components it is common to use ultrasonic inspection to check for defects. Often a zero defect mockup is created. The oscilloscope signals detected on the mockup are then compared against the signals detected during inspection of the manufactured components. If the results differ from those observed on the zero defect calibration specimen, then one can conclude that the manufactured piece is not like the zero defect mockup. If only a zero defect mockup is created and compared against then it is unlikely that inspectors can decipher the nature of a flaw, if present, since different flaws will result in different results due to differing signal interactions. It becomes intuitively logical that several mockups with built in control defects would be useful. The challenge with manufacturing control defects in mockups is simply due to the limitations of manufacturing components. It is

hard to manufacture components with cracks and other such defects in the exact orientation and quantity that one desires.

As a simplified example, if we assume that there are 10 different flange types currently in service on an offshore platform. If we also assume that each flange type has 3 different degradation *modes* then we need 30 different mockups, one for each degradation mode per flange type. This theoretical situation results in a large number of mockups. In reality there are many more flange types and each, in theory, has an infinite number of degradation modes.

Although inspection service providers utilization of phased array scanning on flanges can be useful in identifying what flanges have results that different from that of a zero defect mockup there are significant challenges to accurately identifying the nature of defects that are detected. Simulating the inspection results using finite element analysis software could help bypass the problem of creating several mockups and helps expand the applicability of ultrasonic scanning for condition monitoring of in-service static assets.

4. Hypothesis and simulation scope

4.1. General

By utilizing FEA based simulation tools for ultrasonic inspection that allows for reasonable modeling of flanges, differences in inspection results should be detectable for varying degradation profiles. Simulations will be run for flanges with no defects and can then be compared against those with defects. It is also hypothesized that simulation results for different degradation profiles should also be unique in macroscopic character. These unique differences might then be used as a "fingerprint" for the specific degradation profile. The primary goal of this paper is to explore the possibility of identifying unique macroscopic characteristics in the inspection results that can then be used to differentiate differing degradation profiles from one another. In reality there is an infinite number of degradation profiles. Due to time limitations and access to computational capacity this paper will limit the degradation profiles to interpretations of widely used standard practice guidelines outlined by major oil operators in the NCS. These standards typically specify maximum degradations allowed on in-service flanges. Guidelines usually focus on radial degradation along sealing surfaces and internal degradation, see table 5-1. Accurately modeling the flaws in the simulation software will vary in difficulty depending on the capabilities of the simulation software (CATTIAUX and SOLLIER, 2011). The primary goal of this paper is to show that different degradation profiles can, indeed, result in marked differences in inspection results. Exhaustive efforts to accurately model flaws in the simulation have not been spent. Although exploring the modeling techniques to accurately simulate flaws is indeed vital. As such, the simulation models will utilize simple and rudimentary representation of flaws. The simulation software utilized for this paper is explored in more detail in the next section.

4.2. Flange types and degradation profiles

Simulations will be run on ASME B16.5 300 class RF flange types, see figure 3-1. The RF flange is characterized by a flat sealing surface that is in contact with a spiral wound gasket.

Degradation profiles modeled for the RF flange based on acceptance criteria outlined in typical NCS operator guidelines and technical requirements.

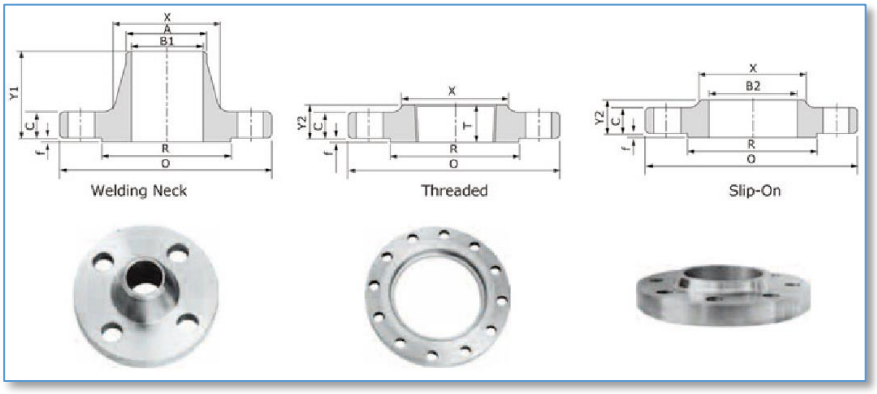

Figure 3-1: RF flange with flat sealing surface profile

5. Applicable simulation tool

There is a wide array of FEA software tools for different applications currently in use today. Several software suits are tailored for specific applications while others allow for a more general range of applications. Some examples of FEA software work environments are electromagnetic, fluid, structural, and thermodynamic. CIVA 11 is a software suit created by EXTENDE[3]. In collaboration with EDF[4] a FEA add-on called ATHENA 2D was created for CIVA 11. The CIVA 11 UT software suite is tailored specifically as a semi-analytical analysis tool for ultrasonic NDE. Although there are add-ons made for a wide range of NDE methods this paper will focus on the ultrasonic NDE, CIVA 11 UT, package with the ATHENA 2D finite element analysis add-on. The ATHENA 2D add-on serves to augment the semi-analytical capabilities of CIVA 11 in modeling complex phenomena that might occur during ultrasonic inspection. This results in a hybrid combination analysis that can run well without the need of excessive computational demand.

The CIVA ATHENA 2D suit allows the user to reduce computational loads and memory burden by specifying a FEA box around an area of interest. The semi-analytical capabilities of, the standalone, CIVA UT software suit calculates the ultrasonic beam propagation up to the FEA box of interest. The ATHENA 2D add-on serves to run further computations within the FEA box using the incident beam, calculated using the semi-analytical methods, as boundary value inputs for the FEA analysis. FEA within the designated box will simulate the ultrasonic beam's complex interactions with defects and specimen geometry. In essence, this combination of semi-analytical and FEA optimizes the simulation and allows the software to be run on computers with relatively limited processor capacity relative to high performance computers specifically designed for simulation (MAHAUT et al, 2010). As the FEA portion of the model requires far more computations than the semi-analytical portions of the model, reducing the area of the FEA box minimizes computational load. Placement of the FEA box should take into consideration the limitations of computational capacity and required accuracy of simulation outputs. The light blue region in figure 4-1 indicates the semi-analytical region and the red region indicates the FEA

[3] EXTENDE Company is involved with research that seeks to merge the benefits of simulation and modeling to the advancement of NDE techniques. It is the developer of the CIVA software suite.

[4] Électricité de France S.A. or EDF is a French electric utility company producing most of its electricity from nuclear energy.

region. Note that the light blue area should ideally only represent areas where complex beam interactions are at a minimum. This helps to ensure the accuracy of the simulation.

The analysis within the FEA box will seek to account for a variety of physical phenomena with regards to beam to defect interactions. The analysis will account for creeping and Rayleigh waves generated on defects. It will also simulate multiple scattering, the precise response from small defects with respect to the wavelength of the ultrasonic beam, and also computes interface echoes. Relevant phenomena such as beam interaction with complex geometries, flaws, and multiple defect clusters are accounted for accurately if specified by the user before running the simulation (EXTENDE, 2014) (DOUDET et al., 2007).

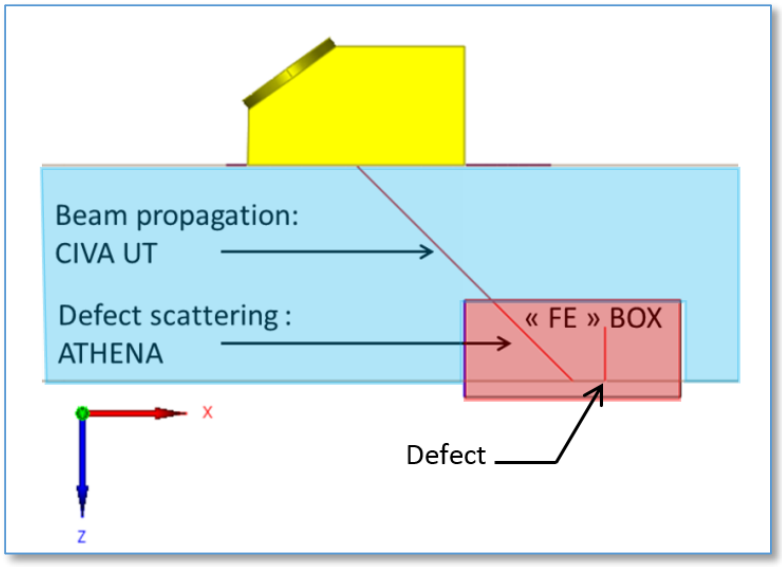

Figure 4-1: Combination of semi-analytical methods and FEA, a hybrid method (EXTENDE, 2014)

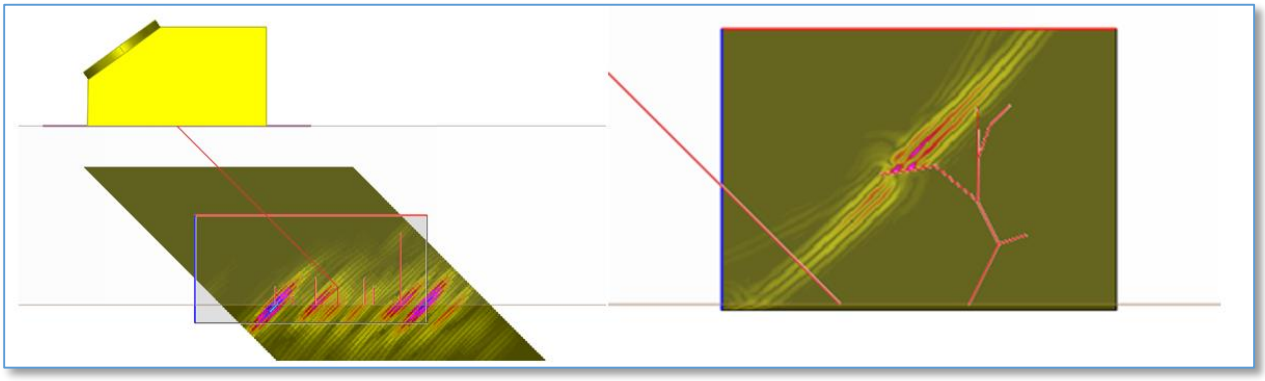

Figure 4-2: The image on the left shows multiple scattering phenomena in a flaw cluster while the image on the right shows the generation of creeping wave phenomena on complex flaws (EXTENDE, 2014)

A potential limiting factor in using the CIVA 11 with ATHENA 2D add-on is that the FEA tools only allow for two dimensional modeling (EXTENDE, 2014). The user must be comfortable with the assumption that the 2D model accurately represents the behavior of the real world application that the user is trying to simulate (MAHAUT et al, 2010). Also, if one is trying to simulate the ultrasonic

behavior of multiple beams, such as phased array ultrasonics, it is worth noting that each individual shot in the array is analyzed individually. Phased array simulation could result in a large computational load.

6. Flange simulations

6.1. Specimen modeling

For the simulation model of the RF flange an ASME M16 5 300 class 8" diameter welded flange was selected. Dimensions for the flange were taken from commonly available tables in supplier catalogues. Utilizing CIVA UT's inspection specimen module to create a Computer Aided Design, CAD, model for the flange cross section, an accurate model for the flange can be generated, see figure 5-1. Although a circular flange can be modeled by rotating the modeled cross section around a radial axis, it is not necessary to model the inspection specimen as a round 3D object since the inspection simulation only assumes a 2D plane of action. In other words the simulated inspection results will not differ weather the specimen is modeled as a circular object or an extruded linear object as long as the cross section is identical. For simplicity the simulation was run assuming a linear extruded component with the specified cross section see figure 5-2.

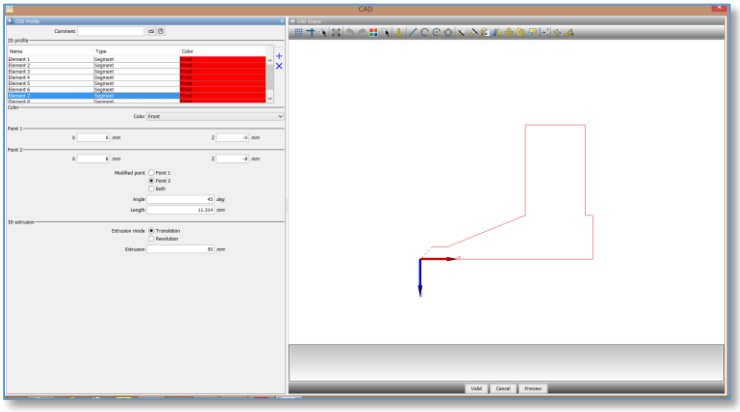

Figure 5-1: CIVA UT specimen CAD modeling. Note that both linear extrusion and circular options available for modeling of specimen.

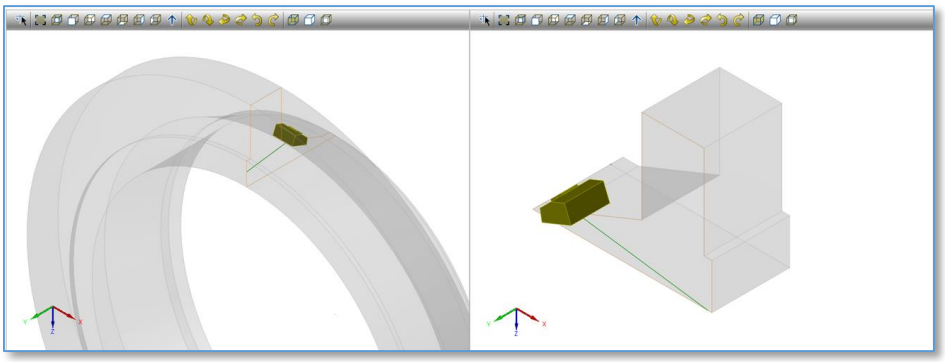

Figure 5-2: Model view on the left shows circular option while the view on the right shows the extruded linear option. The simulation was run on the linear model on the left due to convenience.

Note that manufacturing tolerances were not taken into consideration. The model is based on theoretically perfect geometries.

6.2. Probe parameters

The inspection probe was not specifically modified or modeled to reflect typical probes being used by inspection service providers, but rather optimized to ensure that the beam's travel path would ensure that it reaches the targeted points of interest for the differing degradation profiles. This is simply due to the fact that the primary interest of the simulation is to ensure that the ultrasonic beam will interact with the flaws and regions of the specimen of interest. Probe wedges can be manufactured to suit the specimen of interest and the simulation can also be altered to verify the efficiency of a specific wedge geometry see figure 5-3. CIVA UT allows for a wide array of variables to be specified by the user. Beam signal profiles or crystal geometries can be verified. For this paper the parameters were not changed from their default settings. The primary concern for all the different simulation cases was to make sure that all the parameters are kept the same to ensure that comparisons can be made for like situations that only differ in flaw characteristics.

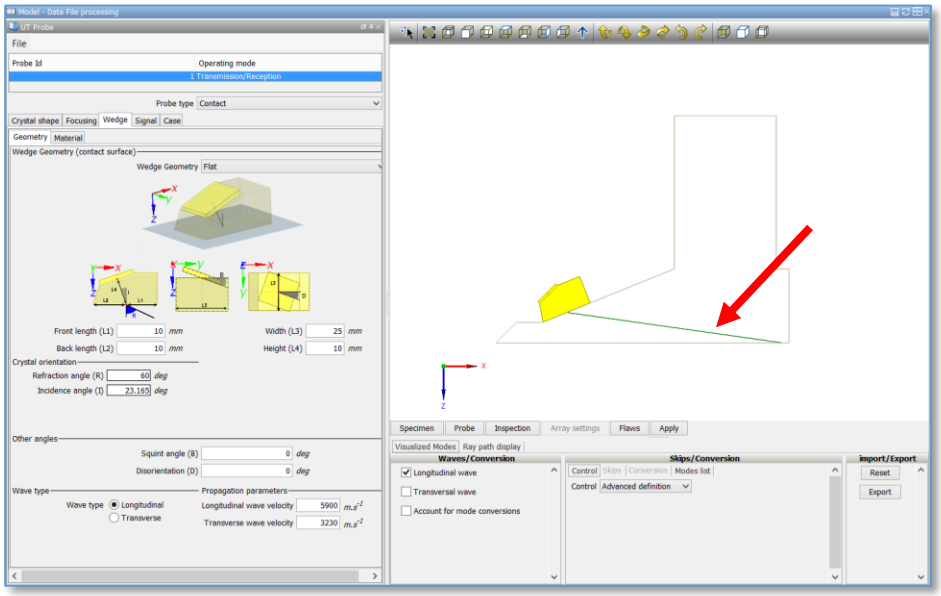

Figure 5-3: Probe wedge geometry. The large red arrow points to the green line representing the ultrasonic beams path of flight from the current probe position on the specimen. The angle can be adjusted by changing the parameters on the left side of the user interface.

6.3. Inspection settings

Most inspection setting parameters that can be modified by the user were left in their default setting. The only specific changes that were made for the simulation was specifying the number of scans to take as the probe traverses the flange neck from its start location. This was done in order to ensure that inspection results could be gathered for a wide range of probe placements to ensure that, when comparing results from different degradation profiles, comparisons could be made with readings taken from the exact same probe location see figure 5-4. The simulation was

run with 2mm increments, at 17 repetitions, that would ensure that inspections were simulated from the furthest possible location of the probe down the flange neck and finally as far towards the flange face the probe could be placed. This is necessary to ensure that inspection results can be obtained for a wide region of the sealing face. Simulations were run with probes generating longitudinal waves as opposed to transversal waves.

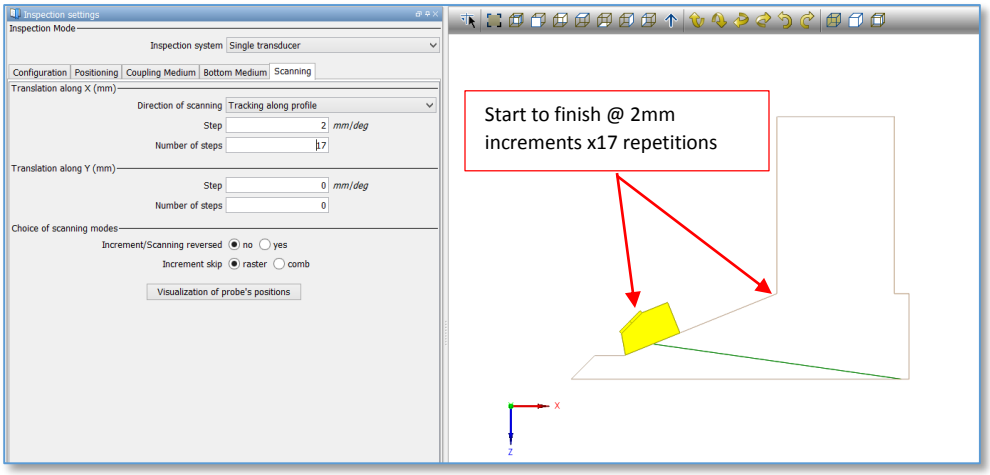

Figure 5-4: Number of scans to simulate along the flange neck

6.4. Simulation settings

Athena 2D allows the user to specify whether or not the simulation should take into consideration signal mode conversions. Although taking into consideration signal mode conversions in the simulation could result in more realistic simulation outputs it does put an additional toll with respect to computational load. The simulations for this paper were run on a standard laptop PC with 8 gigabyte RAM capacity. In order to ensure that the simulations were small enough for the laptop being used, mode conversions were not taken into account. Signal waves for the simulation were arbitrarily designated as longitudinal while backwall reflection and direct mode were also selected.

Simulated Degradation profiles

For ASME B16.5 300# class flanges a flange cross section proportional to that of an 8” diameter flange was created. A zero defect model and three different degradation profiles were simulated. Table 5-1 summarizes the different degradation profiles.

Degradation Profile	Max Degradation allowed by technical guidelines	Model Views	Comments
Zero defect	None	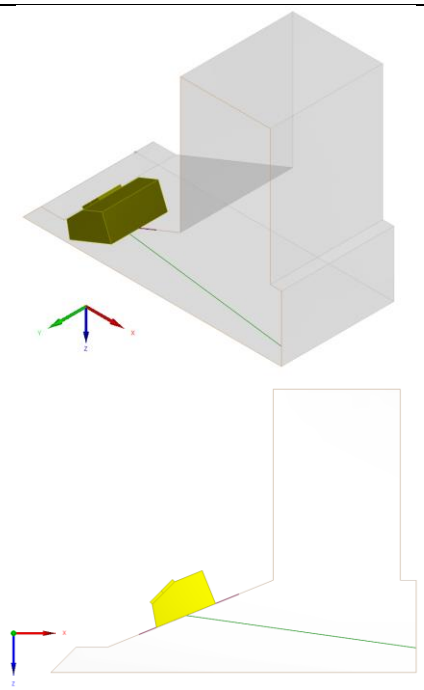	There are no defects modeled in this profile. Note the green line representing the ultrasonic beams path of flight. Nothing obstructs the beams trajectory to the flange sealing face.
Radial degradation close to bottom	"Damages in the seal faces, measured as a radial projection *, can be accepted if they do not cover more than 30% of the width of the gasket surface. Damages should not be deeper than 5mm" 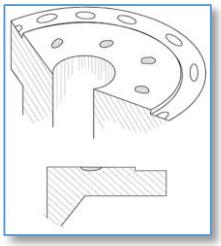	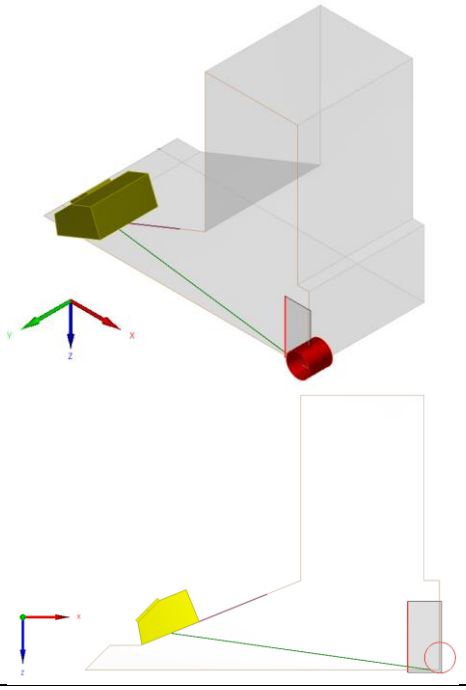	A 5mm deep notch (degradation) is modeled as a circular side drilled hole in the specimen. The total radial length of the flaws combined is roughly 8mm which is about 30% of the gasket surface width.

Radial degradation middle		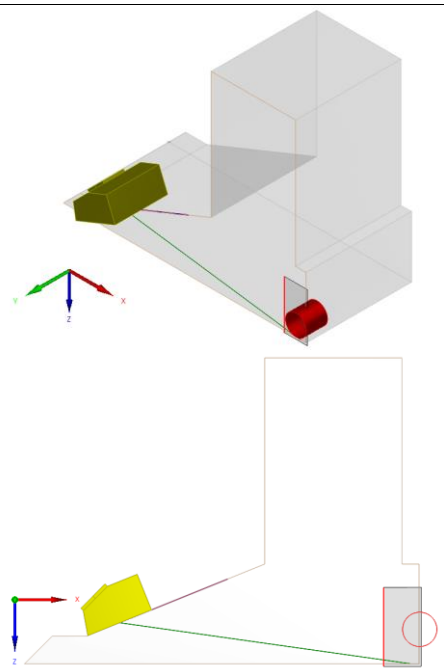	A 5mm deep notch (degradation) is modeled as a circular side drilled hole in the specimen. The total radial length of the flaws combined is roughly 8mm which is about 30% of the gasket surface width.
Internal edge degradation	"Damages of internal edge around the perimeter, may be accepted if they do not cover more than 30% of the width of the gasket surface: BMax = 0.30 x A" $A = \frac{\text{OUTSIDE DIA. RAISED FACE - INSIDE DIA. PIPE}}{2}$ 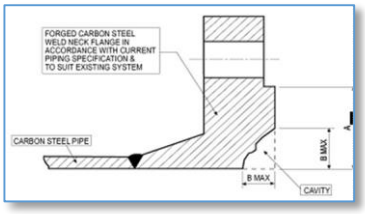	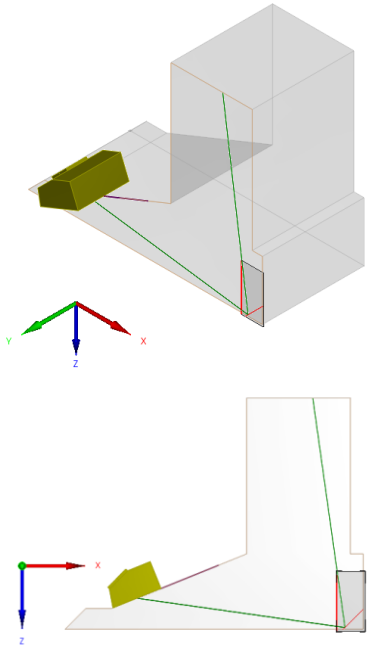	Internal edge degradation is modeled simply as a diagonal obstruction represented by the red diagonal line. Note ultrasonic beams flight of path is affected by the modeled degradation

Table 5-1: RF flange degradation profiles

7. Conclusion

7.1. General

Comparing simulation results for all degradation profiles for an 8" RF flange it is concluded that utilizing FEA simulation might, indeed, be an effective tool in assisting ultrasonic inspectors utilizing standard ultrasonic NDE methods, see chart A-5. Simulation results indicate that specific, macroscopic, signal characteristics can be extracted for different degradation profiles resulting in signal "fingerprints" that can be compared against when performing real life in-service inspection of RF flanges, see figure 6-1.

It should be pointed out that further studies should be performed to verify several assumptions and simplifications that were utilized for this paper. A more extensive discussion is presented in Appendix B. In summary, the following aspects or topics should be studied

Aspect/Topic	Why?	How?
Realistic degradation modeling	This paper assumed rudimentary representation of degradations. Degradations should be properly modeled to verify the degree to which small variations in degradation characteristics affect results. Only by modeling realistic degradations can they be properly verified against actual real flanges with said degradation.	Run more simulations with accurate CAD modeled degradation geometries.
Compare simulation results against real inspection results	Verifying the degree to which a 2D FEA model represents a curved real 3D object will need to be verified.	Compare simulated inspection results against like kind real world inspection results.
Optimize placement and sizing of FEA box	Placement of FEA box and sizing were not scrutinized beyond meeting the limited computational capacities of a laptop PC. Placement of the FEA box is vital, and further studies should verify that there are no other actions present within the test specimen that alters the behavior of the ultrasonic wave fronts within the FEA box. Optimally, the larger the FEA box the better, given that the flange cross sections are complex and signal wave fronts can interact with component geometries outside of the FEA box.	Run simulations with a more powerful computer and maximize the FEA box to encompass as much of the flange cross-section as possible. Compare against results utilizing smaller and smaller FEA boxes until an optimized size is identified.
Study other forms of model variability such as manufacturing tolerances	See appendix B	See appendix B

Model real probes	An inspection service provider's inspection team might not have the ability to purchase new probes. Might be a significant cost saver to utilize existing probes.	FEA model should be modified and run with applicable probes.

7.2. Hypothetical test case

A hypothetical in-service inspection was modeled with a hypothetically unknown degradation profile, see appendix B. Although the inspection results were also an extraction of a simulation utilizing CIVA, it can be concluded that generalized degradation profiles can serve well when categorizing real world results. This statement holds true given the assumption that the simulation results, do indeed, represent accurate real world inspection results for the specific modeled inspection. This assumption should be further verified as discussed in appendix B.

7.3. CIVA UT Athena 2D

CIVA UT along with the Athena 2D add on proved to be a good software tool to explore the potential benefits of incorporating simulation techniques for in-service inspection. The intuitive user interface and ability to import CAD models both for the inspection specimen and the degradations provides an adaptable and user friendly platform. More work remains to verify the accuracy of the 2D simulation results against a real 3D object with curved geometries such as nozzles and pipe flanges, see appendix B.

7.4. Applicability

Given that complex signals resulting from standard ultrasonic NDE on complex components are not verifiable, against a like for like calibration specimen, simulation software might prove to be an added benefit in reducing the need for calibration blocks. Results from this study show that modeled degradation profiles do indeed show characteristic, macroscopic signal, "fingerprints" that can be utilized to categorize in-service flanges into potential degradation profiles. Given that a set of in-service flanges are inspected using ultrasonic NDE the results can be compared against reference charts extracted from simulation tools. Once the comparisons are made, a selection of potential degradation profiles can be identified that might correlate with the actual condition of the inspection results from the in-service flange. These flanges can then be referred to when planning visual inspection scope for the next planned plant shutdown. This will allow the inspection planners to be more selective when planning flanges for visual inspection. This helps reduce inspection scope and so forth, reduces shut down duration.

The potential benefits of FEA simulation are not limited to flanges. There are a wide spectrum of in-service components with a product containment function that have complex geometries that could benefit from the utilization of FEA simulation, see figure 2-3. Expanding the applicability of standard ultrasonic NDE to these regions could result in wider commercial application of current capabilities.

8. References

- BURCH S.F., COLLETT N.J., 2012. *HOIS Recommended Practice for in-service inspection of RF flanges faces using phased array ultrasonic techniques*, HOIS(11)R7 Issue 2
- MAHAUT S. et al. 2010. *Simulation of complex ultrasonic NDT cases using coupled analytical-numerical method*: The MOHYCAN Project
- CATTIAUX G. and SOLLIER T. 2011. *Numerical simulation of nondestructive testing, an advanced tool for safety analysi*s. Institut de Radioprotection et de Sûreté Nucléaire (IRSN), Reactor Safety Division.
- CIVA ATHENA 2D, Avaliable from: <http://www.extende.com/civa-2/civa-athena-2d>. [10 February 2014]
- SEGERLIND L.J., 1984, 'Applied Finite Element Analysis', 2nd edn, John Wiley & Sons, Inc., Hoboken, NJ, pp. 165-176.
- GENGEMBRE N. and LHEMERY A., 2000. *Pencil Method in Elastodynamics*. *Application to ultrasonic field computation*, Ultrasonics, vol 38, p.495-499
- DOUDET L., CHASSIGNOLE B., DUPOND O., 2007. *Influence of crack networks on the Ultrasonic Inspection of a Propagated defect*, Proceedings of the 6th International Conference on NDE in Relation to Structural Integrity for Nuclear and Pressurized Components.

9. Bibliography

- LOLAND A., and LID P.A., 2010, 'The NDT Handbook', FORCE Technology Training Norway AS, Brøndby, Denmark.
- CHEN H. D., WANG Y. W., and XUE J. 2004. *Numerical Simulation of Ulrasonic Non-Destructive Testing for Welds*. Welding research institute, Xi'an Jiaotong University.
- MARKLEIN R., MAYER K., AMPHA P., and LANGENBERG K. J., 2003. *Computer Simulation of Ultrasonic Non-Destructive Testing of Concrete Using the Elastodynamic Finite Integration Technique (EFIT)*. Non-Destructive Testing in Civil Engineering. University of Kassel Department of Electrical Engineering/Computer Science Electromagnetic Theory, Kessel, Germany.

Appendix A – Simulation results

RF flange results and comparisons

Chart A-1: Degradation profile - Zero defect

	Probe position 1	Probe position 2	Probe position 3
Model	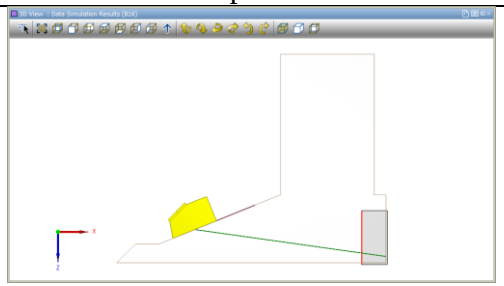	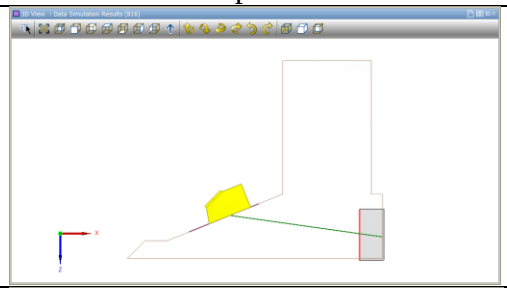	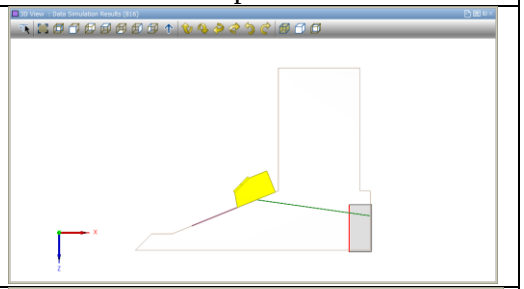
AScan signal amp. vs. time	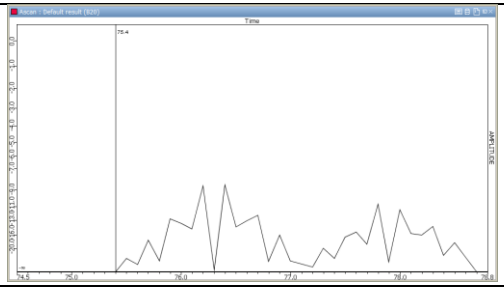	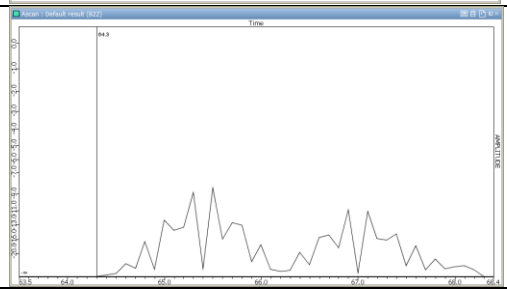	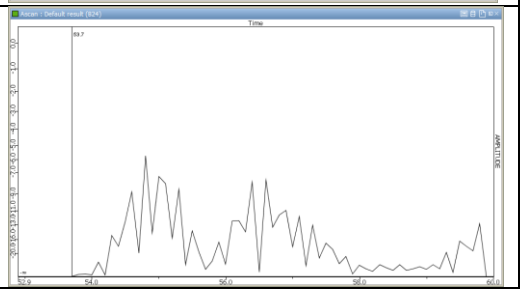

Chart A-2: Degradation profile - Radial degradation close to bottom

	Probe position 1	Probe position 2	Probe position 3
Model	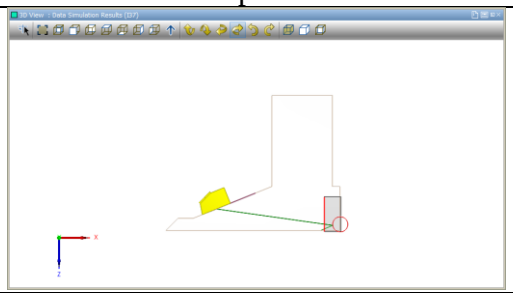	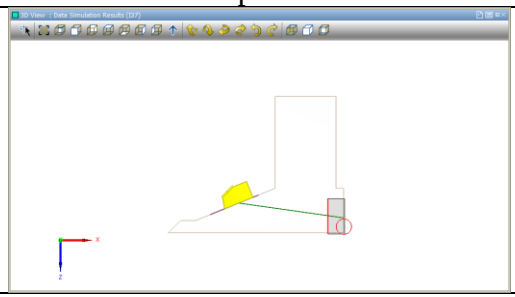	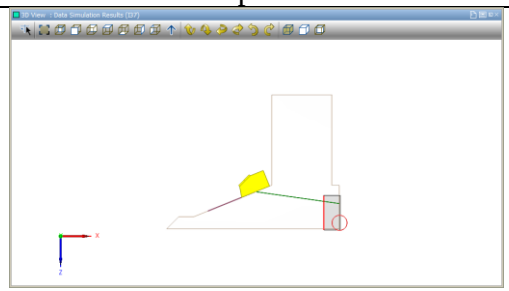

AScan signal amp. vs. time	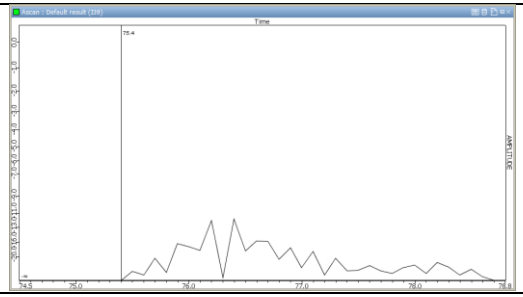	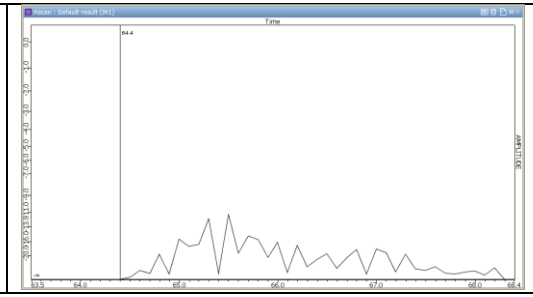	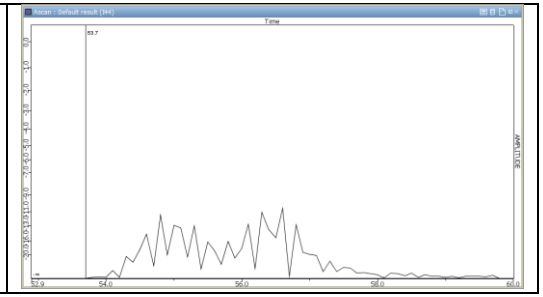

Chart A-3: Degradation profile - Radial degradation middle

	Probe position 1	Probe position 2	Probe position 3
Model	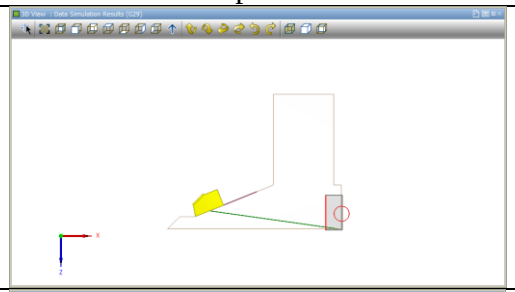	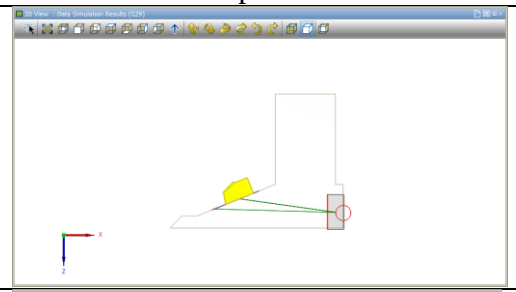	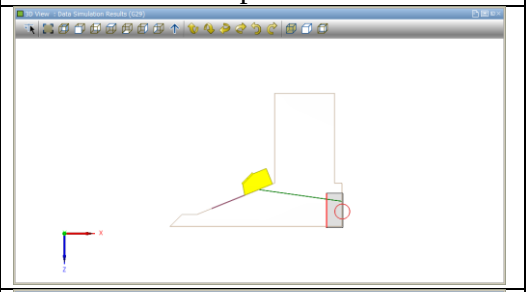
AScan signal amp. vs. time	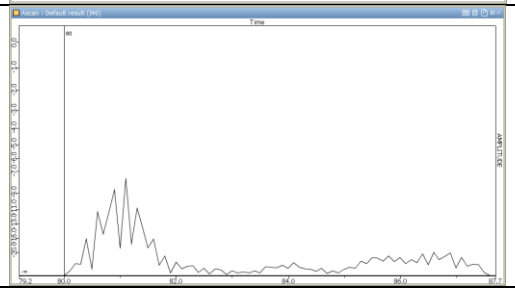	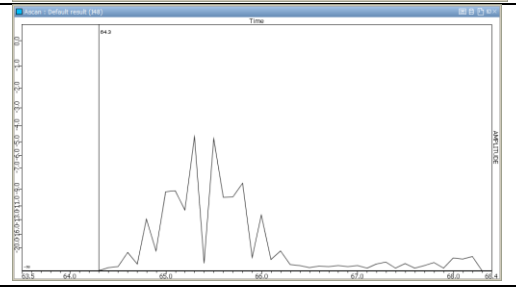	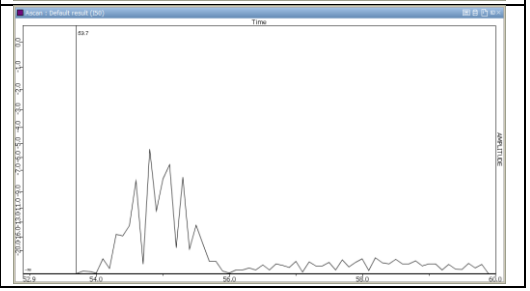

Chart A-4: Degradation profile - Internal edge degradation

	Probe position 1	Probe position 2	Probe position 3

Model	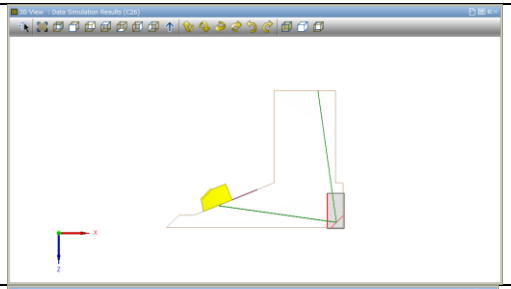	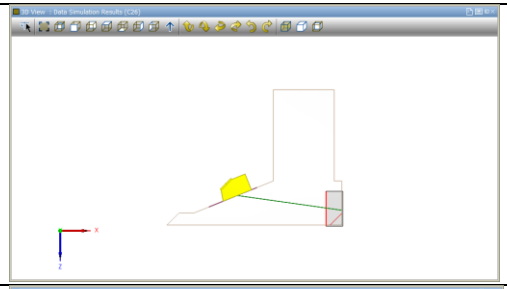	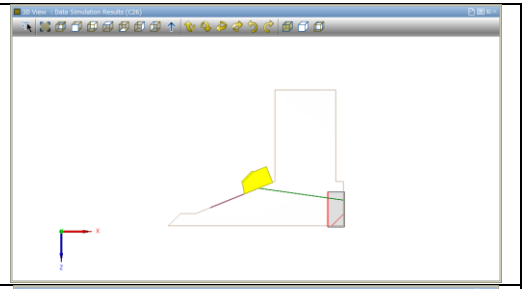
AScan signal amp. vs. time	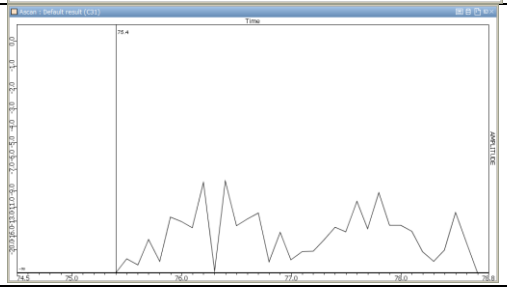	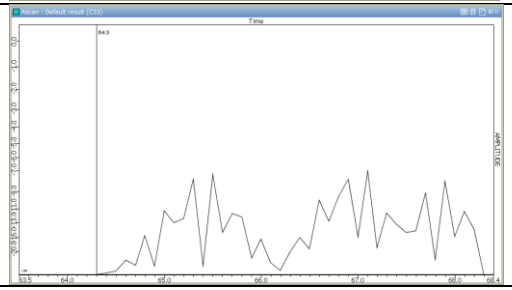	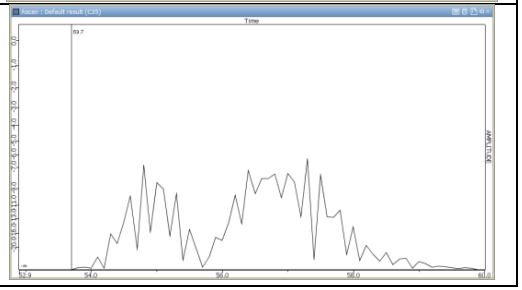

Chart A-5: Result comparison table

	Probe position 1	Probe position 2	Probe position 3
0: Zero defect	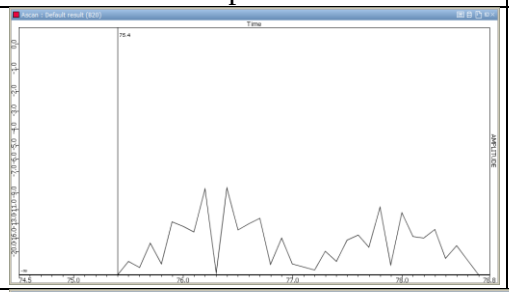	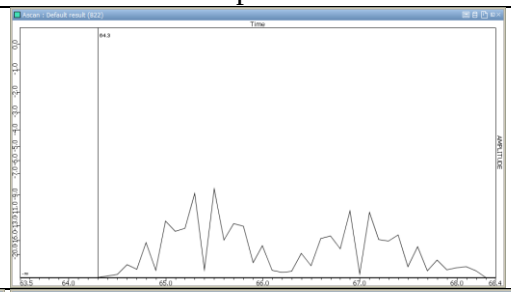	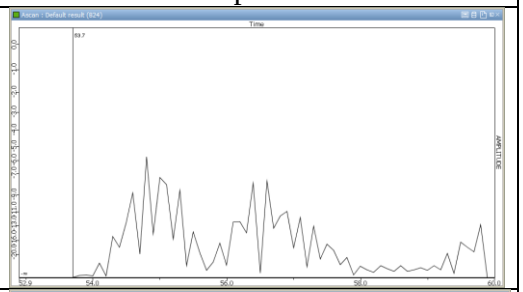
1: Radial degradation bottom	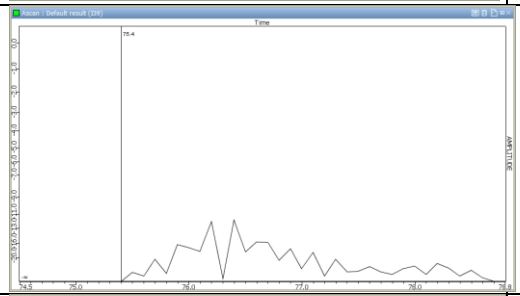	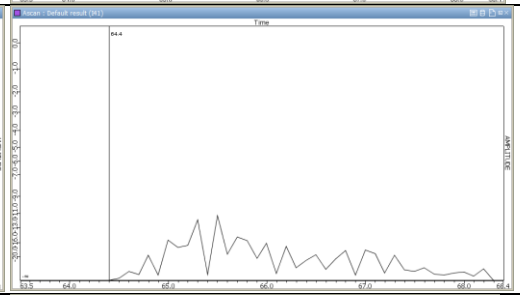	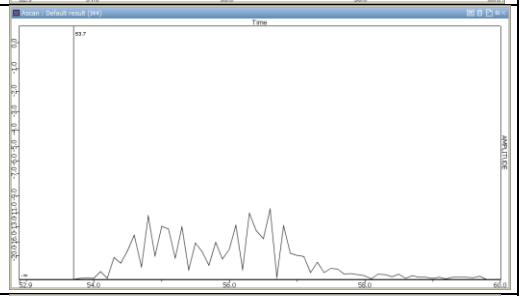
2: Radial degradation middle	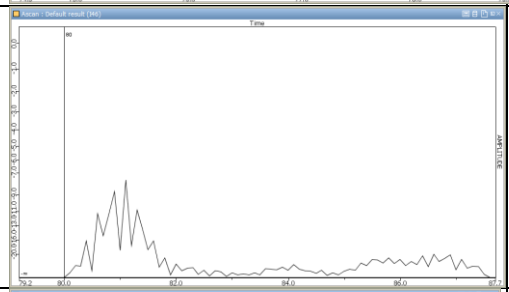	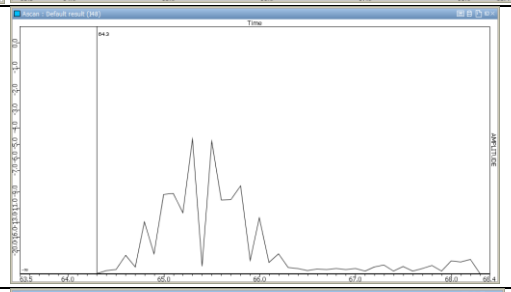	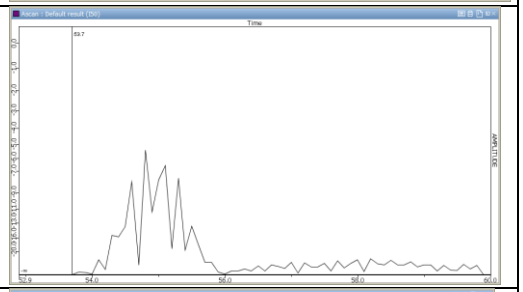
3: Internal edge degradation	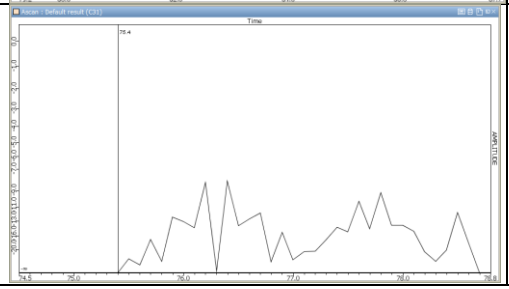	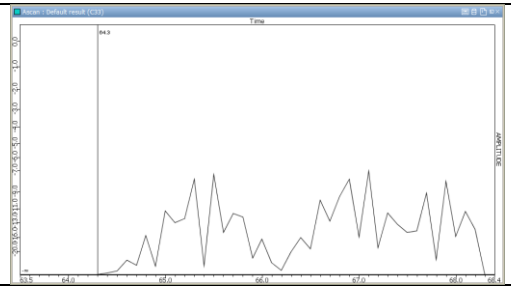	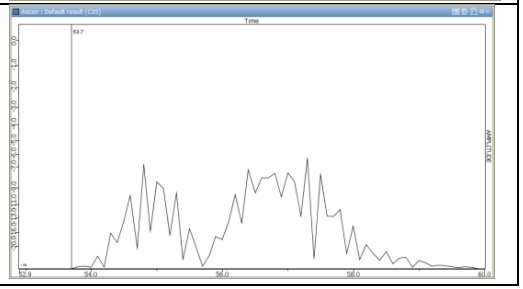

Results from the three different degradation profiles against the zero defect case shows marked differences in the amplitude vs. time graphs. These characteristic differences can be classified as macroscopic characteristics. Some graphs have significantly lower amplitude peaks congested and bound within different points of time. Other graphs show signs of large amounts of wave scatter and interference which is evident in the flatter and longer signal amplitude plateaus. These characteristics are seen on the two radial degradation profiles. The curved nature of the modeled degradation significantly reduces the amount of ultrasonic echo that travels directly back to the inspection probe, see the following chart A-6. Chart A-6 shows wave front field views at different points in time and compares them against the signal amplitude graph for probe position 3. This in turn reduces the signal strength and as such resulting in lower amplitudes on the graph.

Random degradation comparison against degradation profiles:

In this section a hypothetical inspection results from the following case, see figure A-1, was compared against the degradation profile "fingerprints" in order to categorize the condition of the hypothetical in-service flange.

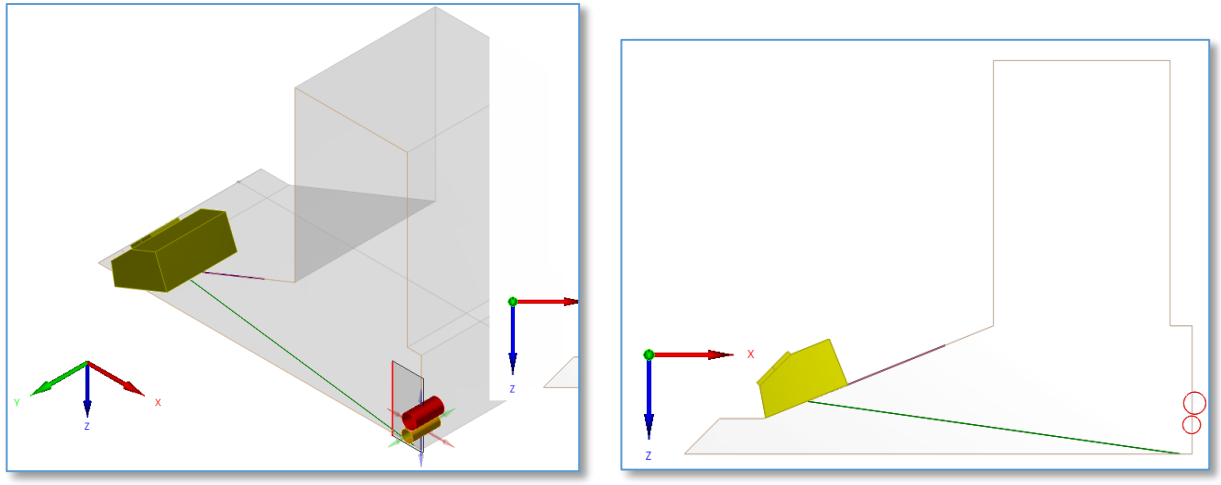

Figure A-1: Hypothetical in-service flange case with two circular degradations clustered on the flange seal surface.

Chart A-6: Hypothetical in-service results

	Probe position 1	Probe position 2		Pro
Hypothetical in-service flange case	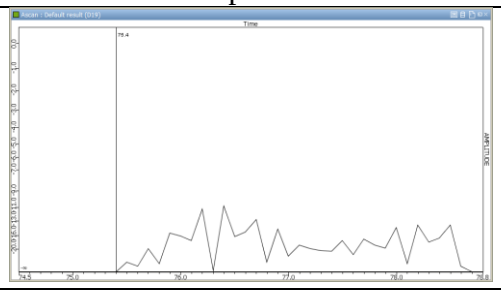	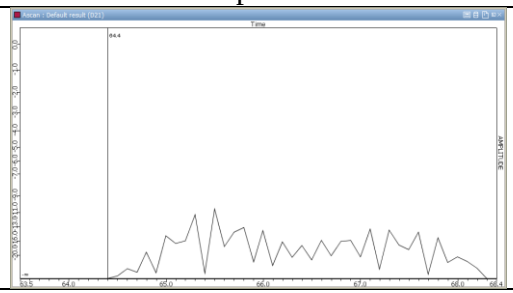	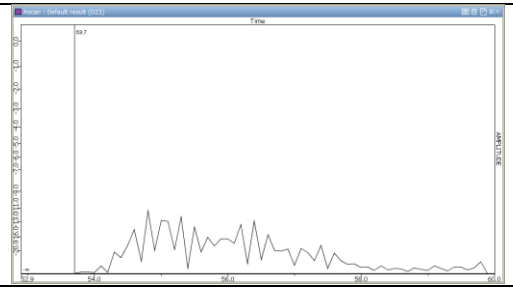	

Looking at the results from the hypothetical case and comparing them against Chart A-5 it becomes apparent that the flange is not in perfect condition. There appears to be a significant difference between the inspection results, for all probe positions, and the simulation results for the zero defect case, primarily with respect to amplitude distributions. This might be a result of signal scatter hinting at possible circular or curved degradation. Further comparisons between the cases are summarized in the following bullet points;

- Position 1: most similar to profile 1 and 3 – radial bottom or internal edge defect
- Position 2: most similar to profile 1
- Position 3: most similar to profile 1

Based on these results with 3 votes for profile 1 and one vote for profile 3 we can conclude that the in-service flange shows signs for a radial degradation close to the bottom of the sealing face. Although the hypothetical in-service senario was meant to represent a radial defect close to the middle of the flange we can see that we were able to successfully conclude that there was a flaw in place and that it most likely is a form of radial degradation. The results are significantly different from the radial degradation middle degradation profile which is quite puzzleling and indicates that further refinement of degradation modeling should be conducted as discussed in appendix B.

Chart A-7-1 Zero defect probe position 3

Image of Field View	Amplitude vs. Time graph
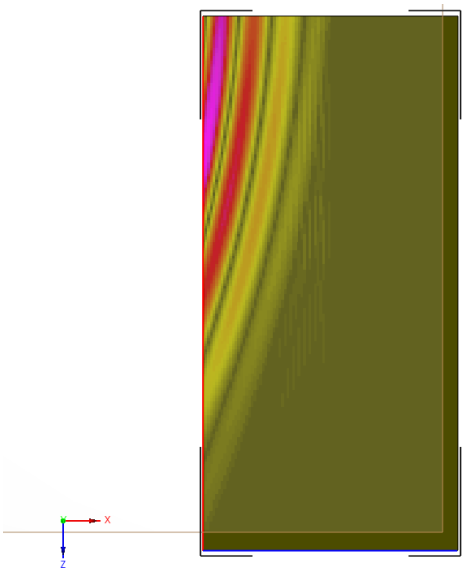	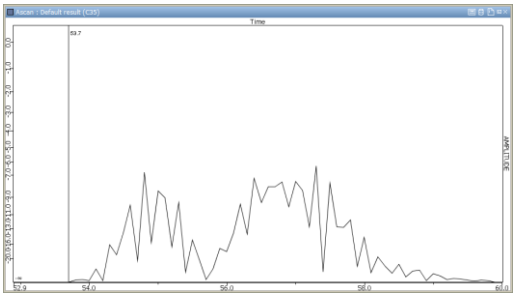
	Wave front is propagating towards backwalls. No signal detected by inspection probe yet.
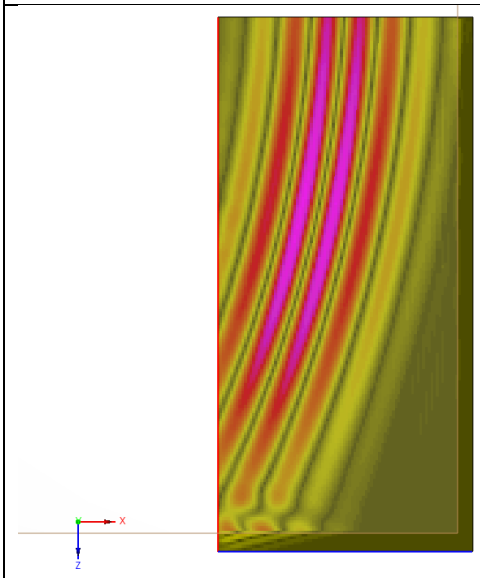	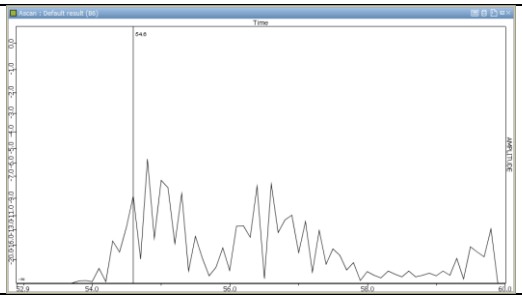
	Amplitude increases as ultrasonic wave front contacts bottom backwall of flange. Contact is visible on the lower left region of the field view.
	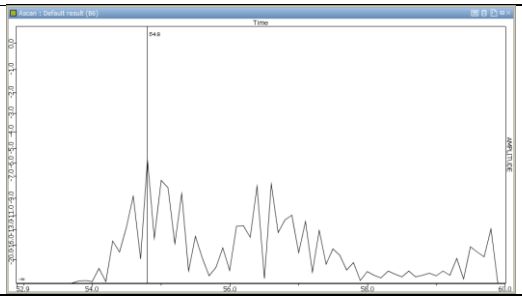

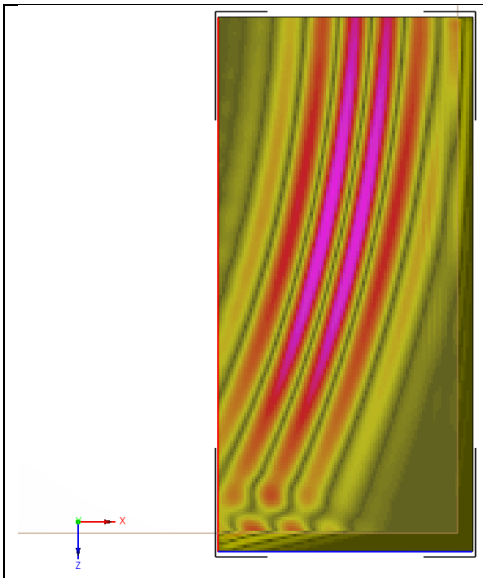

Amplitude increases further as ultrasonic wave front contacts both bottom backwall and upper sealing face. Contact is visible on the lower left region and upper right region of the field view.

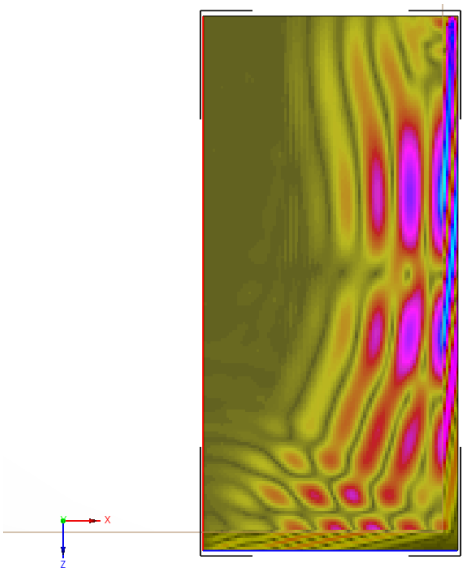

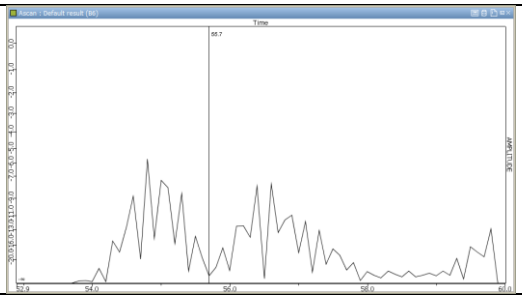

Drop in amplitude as a result of wave fronts canceling each other out. Backwall reflected wave fronts from inner backwall and sealing face are interacting resulting in signal losses. Effects of cancelation are evident in the field view as diamond like or oval like higher amplitude regions emerge. This is due to the cancellation effects of perpendicular collision of two wave fronts with similar amplitudes. Cancelation is concentrated in the lower region of the field view.

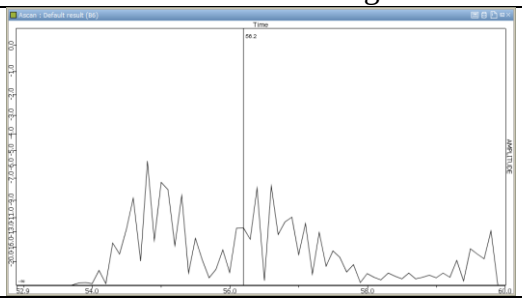

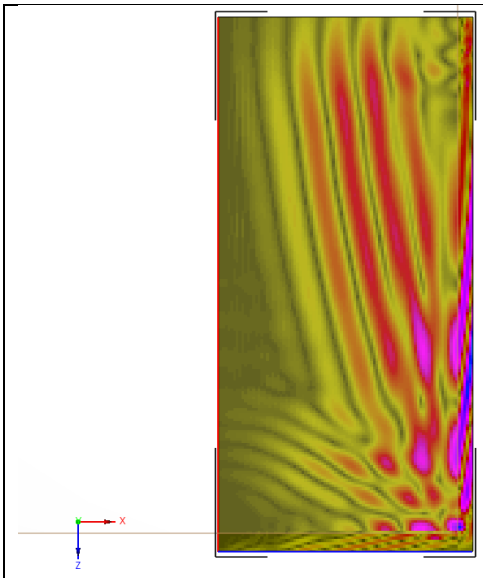

Amplitude starts to increase again as interacting echo wave fronts reduce the effects of cancelation.

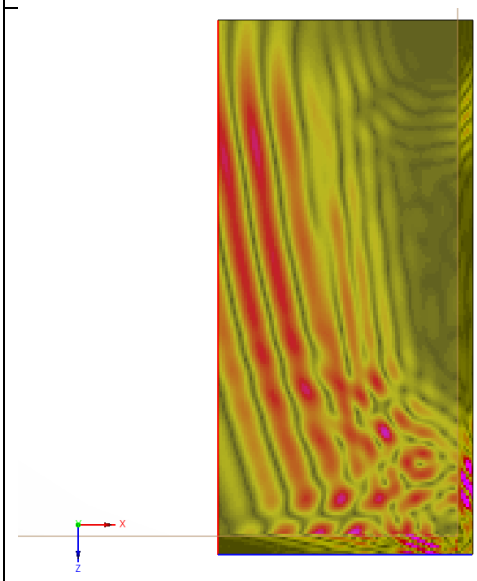

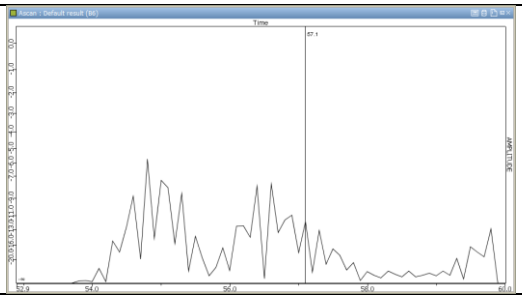

Amplitude drops as wave front is hardly interacting with backwalls and wave front amplitude is reduced due to cancelation effects.

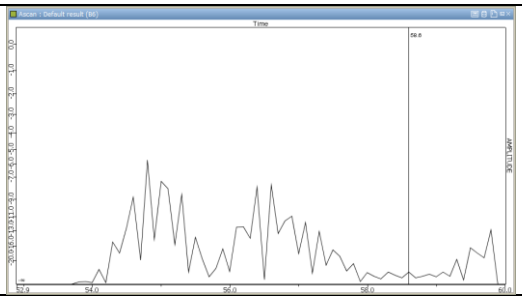

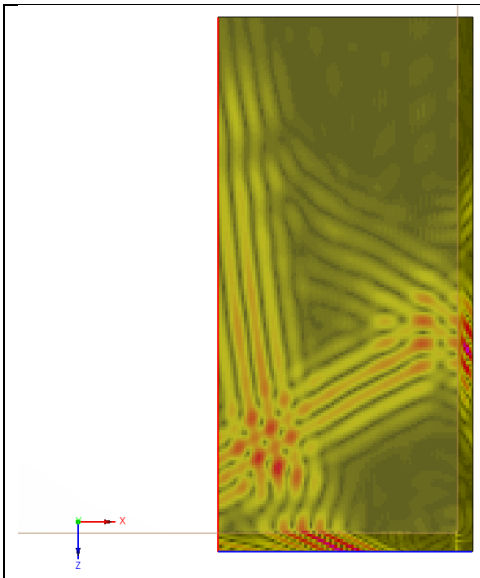

Multiple low amplitude wave fronts resulted from reflections due to backwalls. Signal starts to fizzle out.

Chart A-7-2 Radial degradation bottom from probe position 3

Image of Field View	Amplitude vs. Time graph
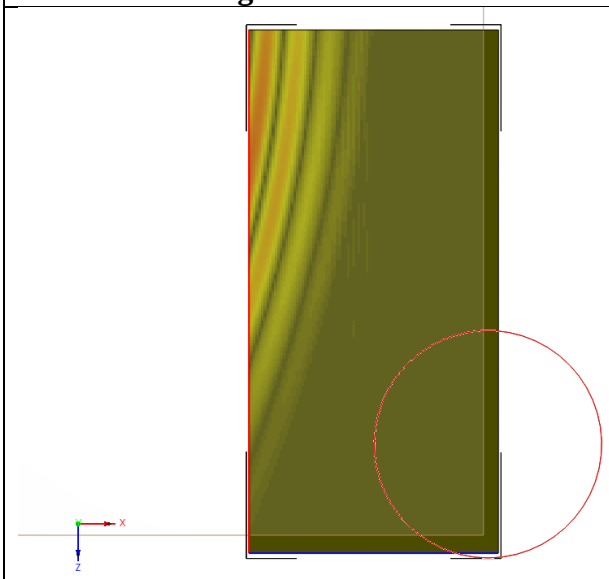	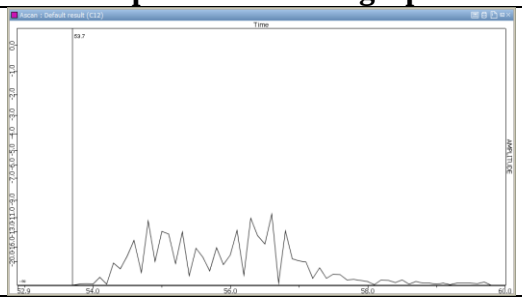
	Wave front is propagating towards backwalls and flaw. No signal detected by inspection probe yet.
	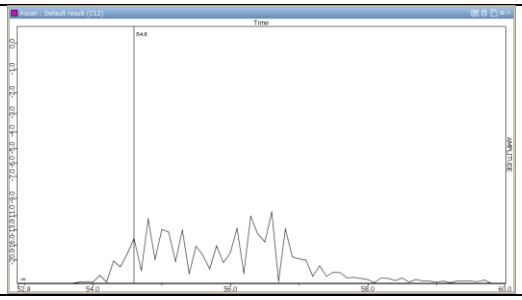

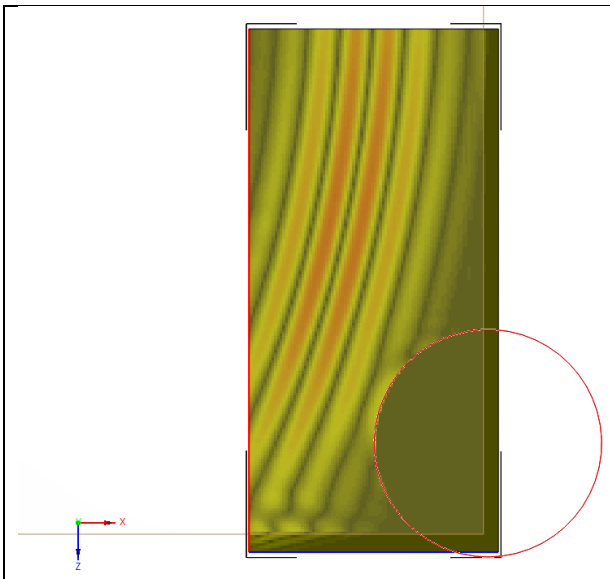

Amplitude is starting to increase as wave front interacts with backwalls and circular flaw.

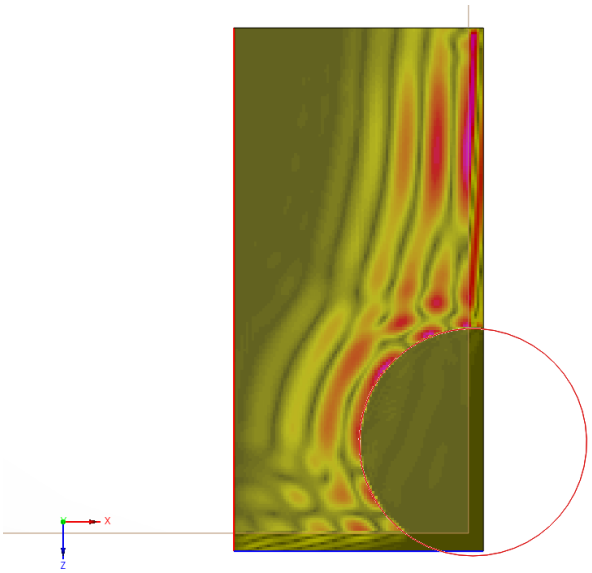

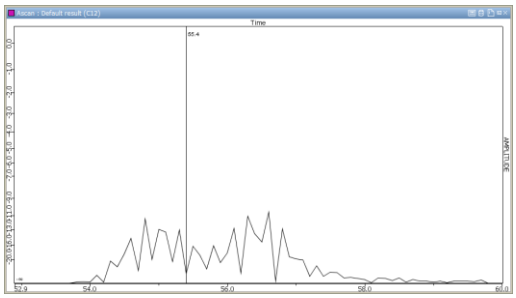

Amplitude slightly dropped as multiple wave fronts in different directions are starting to cancel each other out reducing the signal strength detected by the inspection probe. The average amplitude around this time band is relatively low as a result of a circular defect that scatters waves.

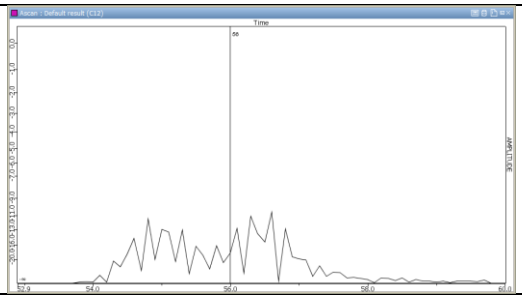

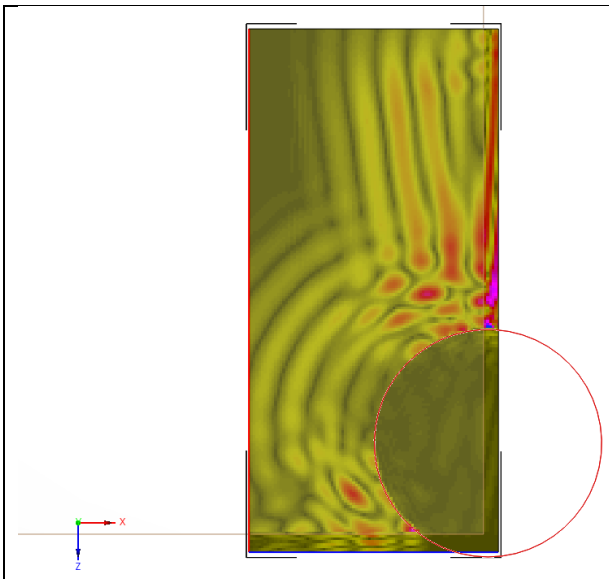

Amplitude starts to increase as wave front further interacts with backwalls and defects but effects of cancelation are reduced.

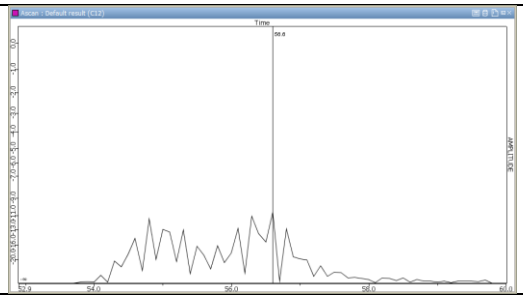

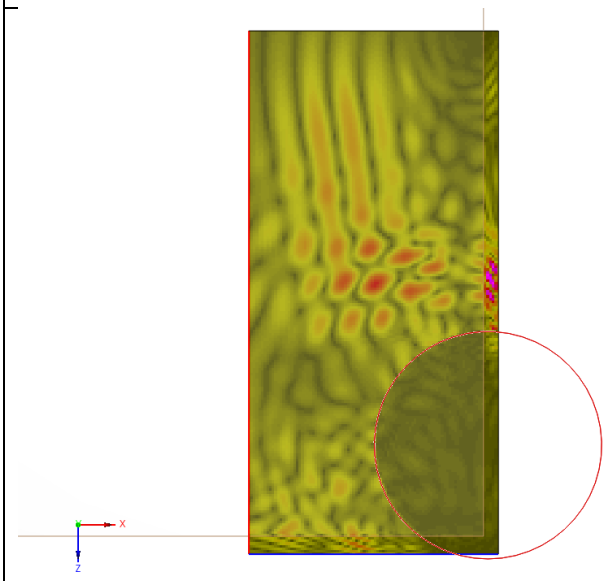

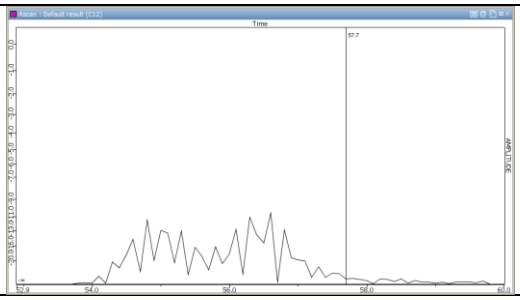

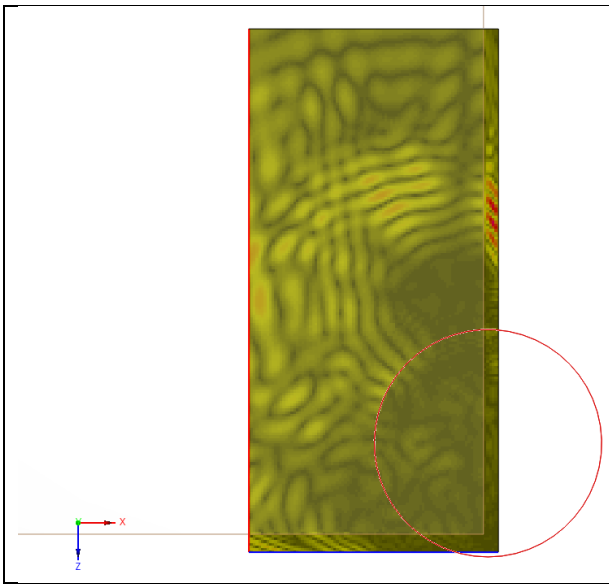	Multiple low amplitude wave fronts resulted from reflections due to backwalls and circular defect. Complex interactions occur due to the curved echo wave fronts from the circular defect. Signal starts to fizzle out.

Chart A-7-3 Radial degradation middle from probe position 3

Image of Field View	Amplitude vs. Time graph
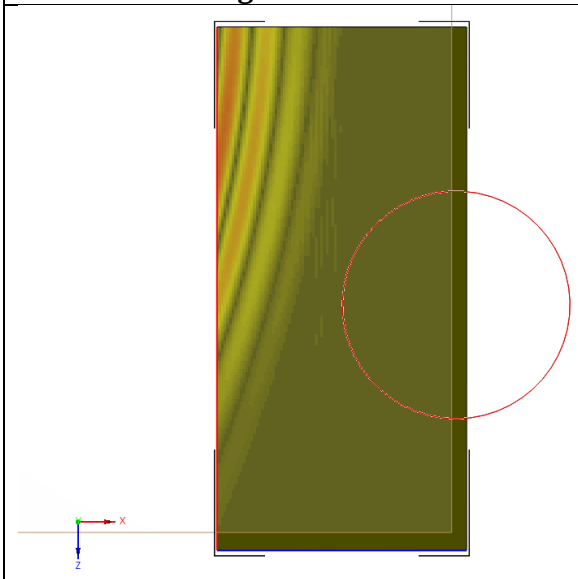	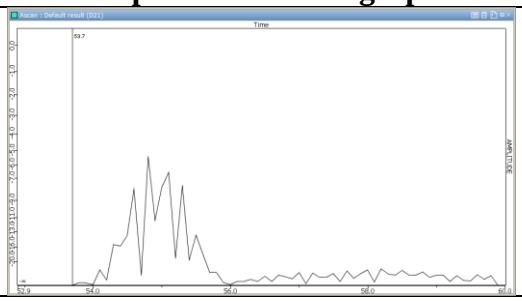
	Wave front is propagating towards backwalls and flaw. No signal detected by inspection probe yet.
	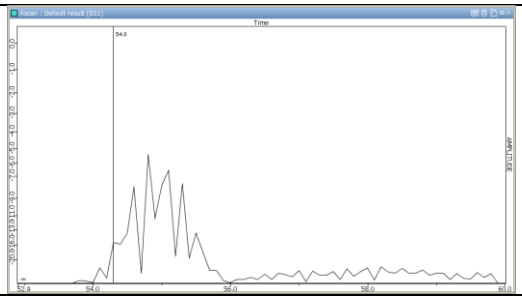

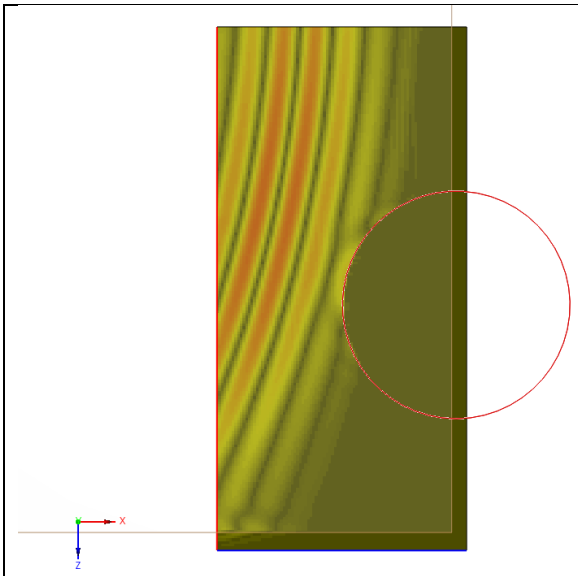

Signal amplitude starts to increase as propagating wave front starts to hit and interact with inner face backwall of flange and circular degradation.

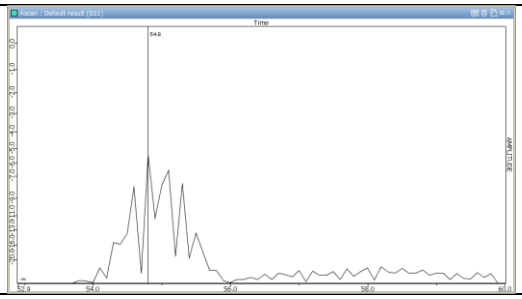

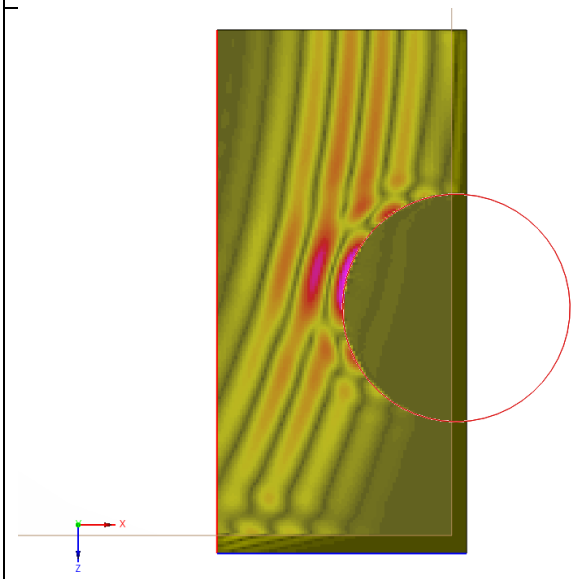

Signal amplitude increases as propagating wave front interacts further with backwalls and circular degradation.

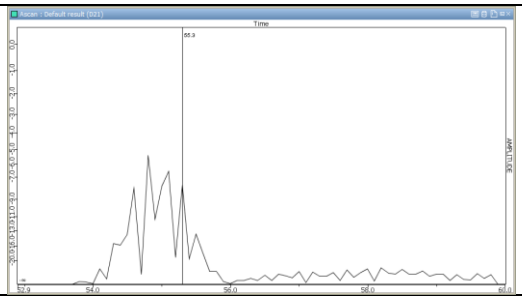

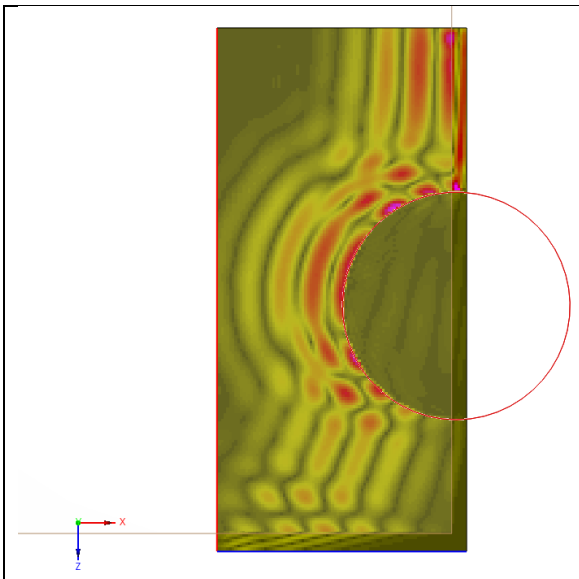

Amplitude slightly decreased as different wave fronts begin to interact and cancel each other out.

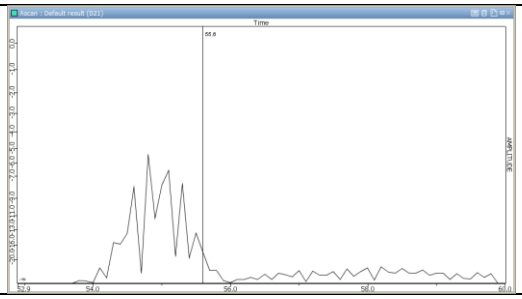

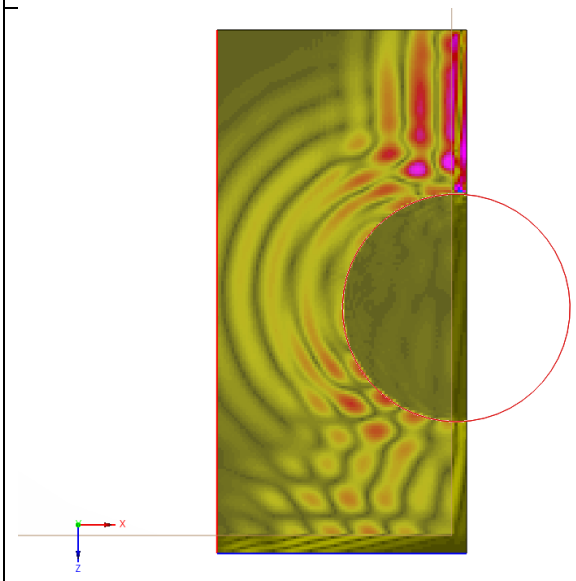

Amplitude on signal quickly drops and fizzles out.

Chart A-7-4 Internal edge degradation probe position 3

Image of Field View	Amplitude vs. Time graph
	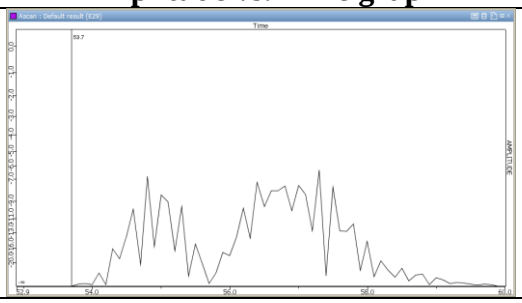

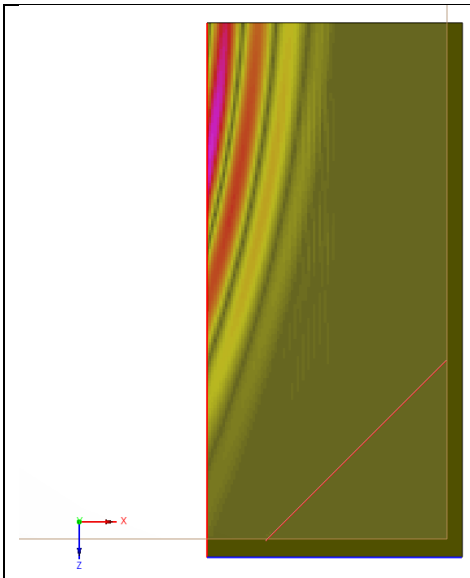	Wave front is propagating towards backwalls and flaw. No signal detected by inspection probe yet.
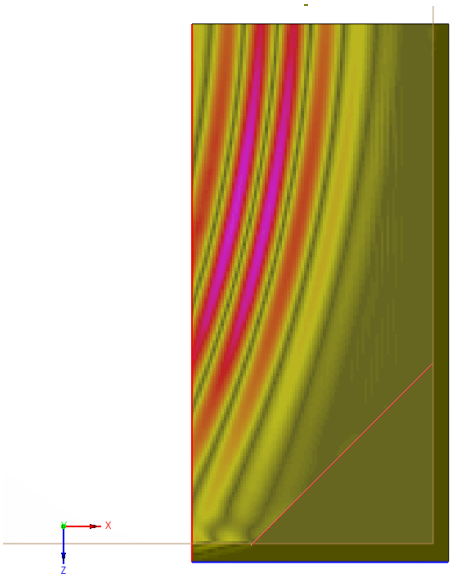	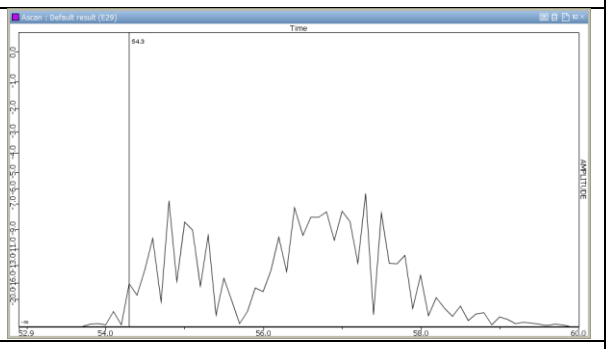 Signal amplitude starts to increase as propagating wave front contacts internal backwall and diagonal degradation profile.
	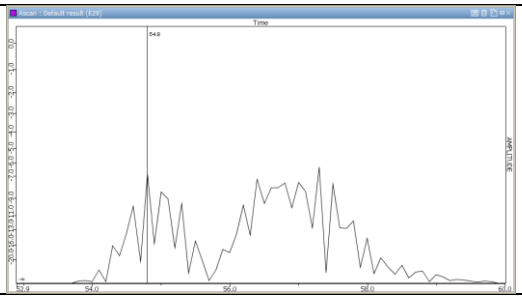

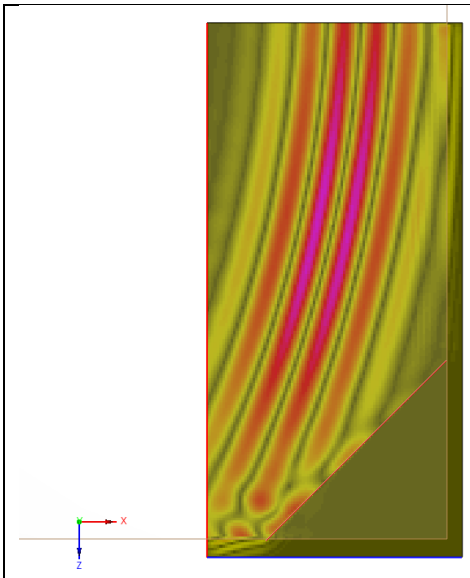

Signal amplitude continues to increase as propagating wave front contacts internal backwall and diagonal degradation profile.

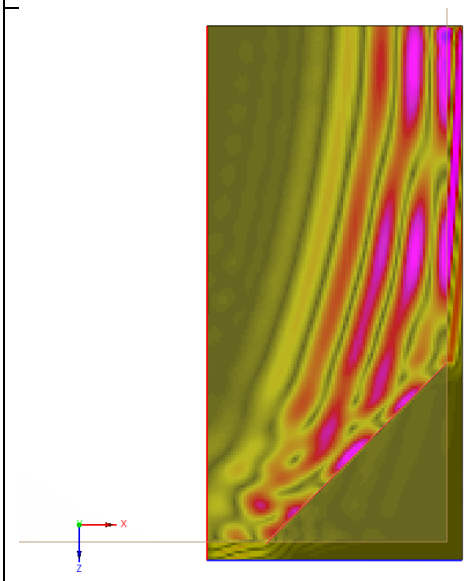

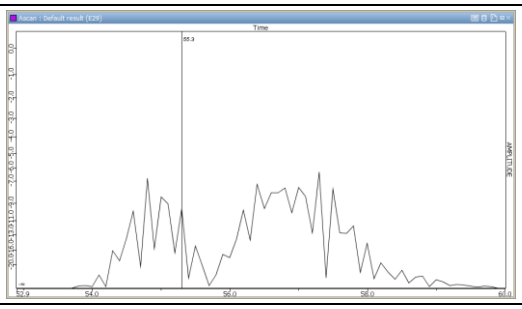

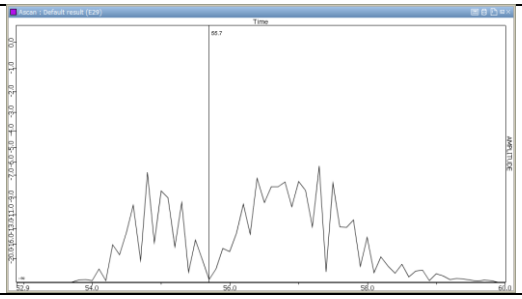

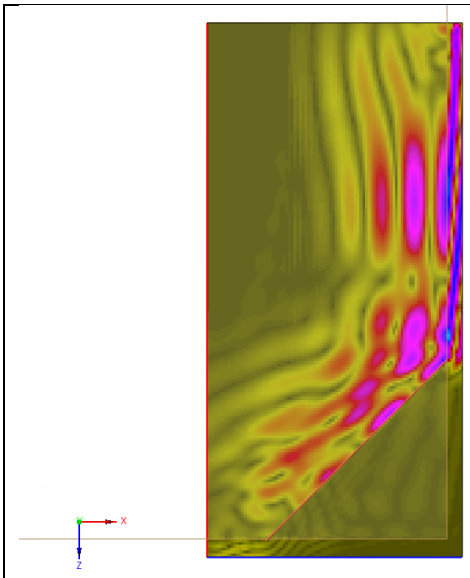

Temporary dip in amplitude as wave fronts from backwall echoes interact and cancel each other out.

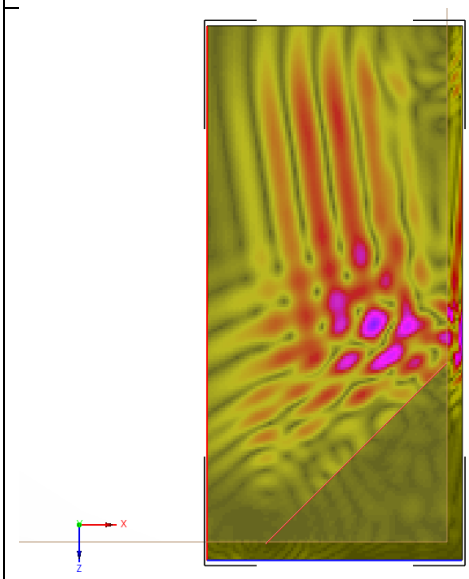

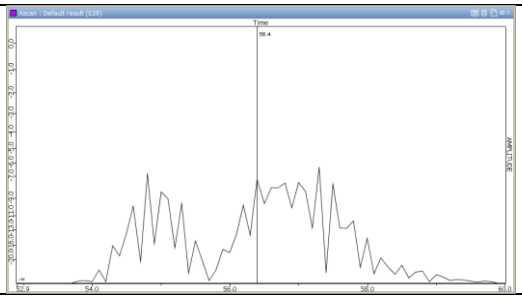

Signal amplitude starts to rise again.

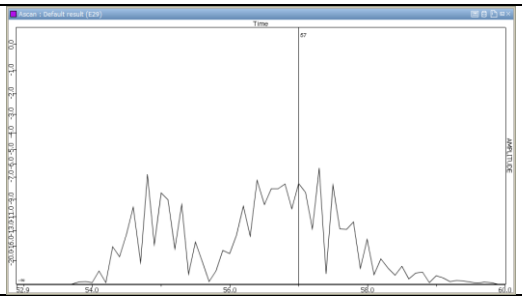

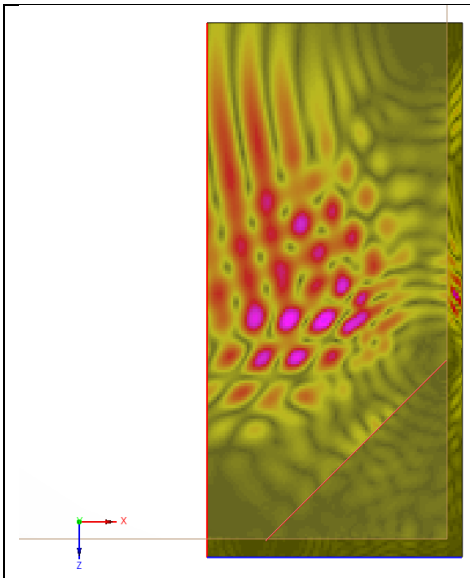

A prolonged period of relative stable amplitude. This might be due to the relative symmetrical arrangement of the simulation and flat defect interfaces resulting in stable conservation of total amplitude.

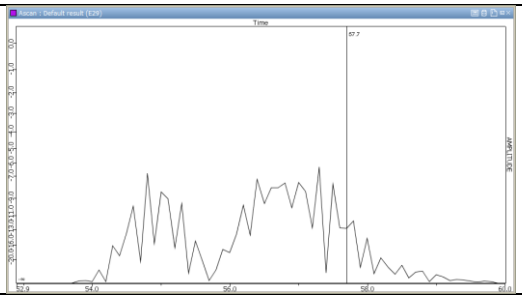

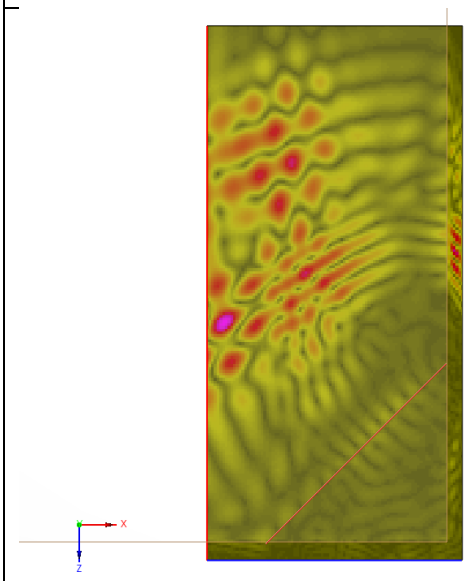

A smooth amplitude decline is initiated

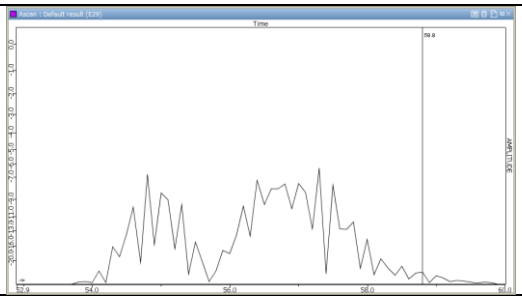

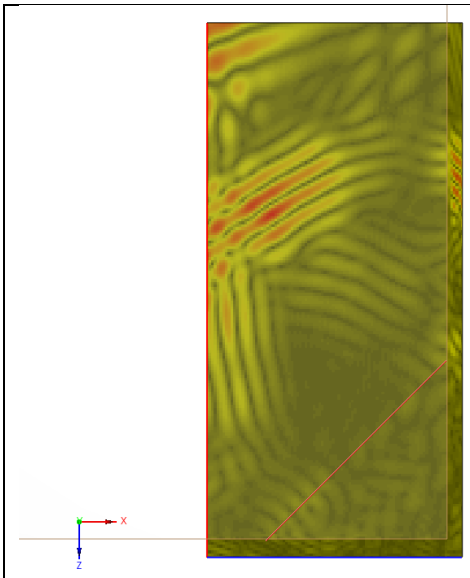	Amplitude on signal gently drops and fizzles out.

Appendix B - Further notes on simulation modeling

Varying the specimen simulation model will usually have a result on the final output of the simulation. Although this paper has not explored in detail the degree to which certain model parameters will affect the analysis output (i.e. the inspection results), it is important to take note of the major variables that should be considered further. In many cases the manipulation of simulation settings, such as probe wedge dimensions, probe placement, probe crystal dimensions, beam focus, frequency, and a multitude of other factors deal with variables that correlate with a desired or optimized inspection procedure. These variables can be modeled in the simulation to further verify the effectiveness of using a certain technique or procedure in correctly identifying the in-service condition of the component being inspected. In other words, it might be possible to simulate several scenarios. From the simulation results, one can identify an optimal procedure for proper flaw detection and characterization. Although the following cases are not exclusive, they do represent some of the variables that could have a significant effect on simulation results.

Ultrasonic probe and signal: A good simulation should allow the user to specify the ultrasonic probe types being used. The simulation should accurately consider the behavior of the modeled probe. Further testing should be performed to compare the different probe characteristics and their ability to differentiate flaw characteristics. Signal pulse characteristics such as length (long vs. short) and the effects of mechanical dampening could also be studies further.

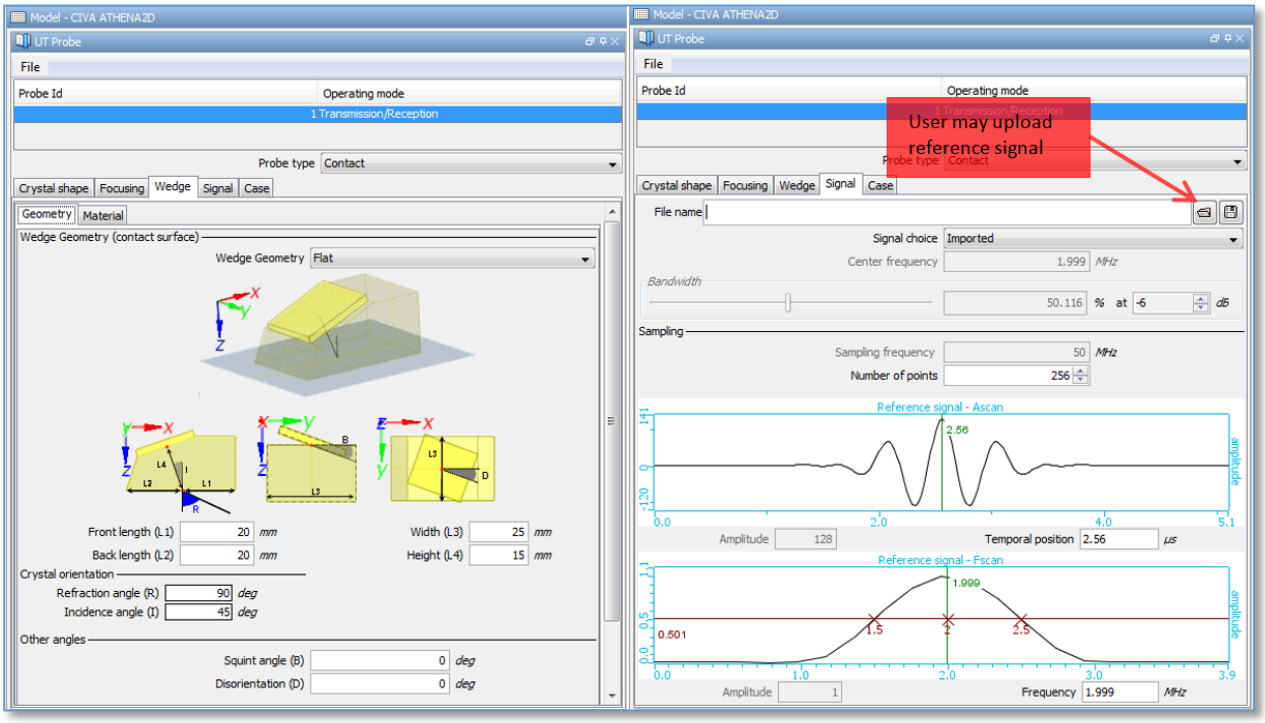

Figure B-1: CIVA UT allows the user to specify a wide spectrum of probe characteristics. Note that even reference signal characteristics can be customized and allows the user to upload profiles. Simulations can be tailored to verify the degree to which probe characteristics has on generating accurate inspection results that can be correctly interpreted.

Flaw characteristics: The degree to which flaw characteristics should be varied to study their effects on simulation results should also be taken into account in further simulations. When considering material losses due to corrosion or erosion the surface characteristics could be relatively smooth for erosion but it could also be rough if the material loss is due to corrosion such as intercrystalline corrosion. Other aspects that could affect the accuracy of simulations is the presence of heat affect zones HAZ if the flange surface has been repaired in the past with welding. The HAZ might have different mechanical properties such as hardness and density which could affect the way ultrasonic waves propagate through the material. This could potentially be taken care of by modeling in a region with different material characteristics that mimic the characteristics of the HAZ. There might also be a combinational affect with both material losses and crack formations which might also have a significant effect on the simulated inspection results. Simulation results comparing the effect of a wide spectrum of flaw characteristics should be looked into.

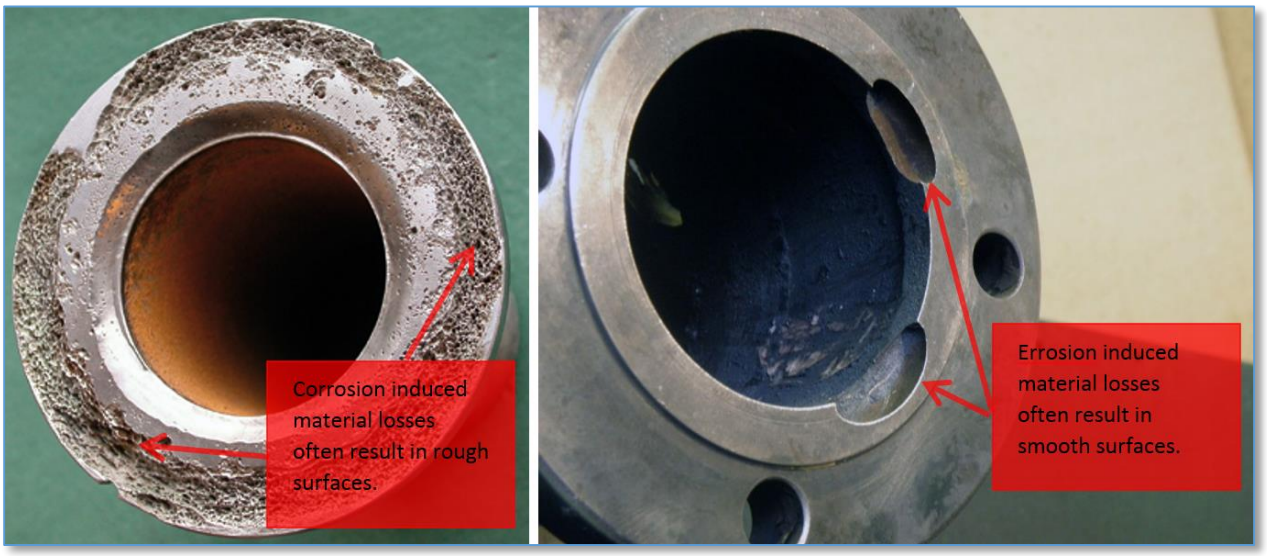

Figure B-2: Rough boundaries profiles compared to smooth boundary profiles generate more beam scatter affecting inspection results. The degree to which the beam scatter affects the final inspection results should be further studied.

As evident from figure B-2 corroded degradations result in rough and variable surface characteristics unlike smoother surfaces that are a result of erosion. Modeling these variable characteristics was not attempted in this paper. Further studies could potentially look at the degree to which a generic representation of a degradation type can be represented in a simplified manner for simulation. There might not be a time saving and simplified manner to model the flaws without major compromises in the results when compared to results from a real world inspection. If that is the case then modeling degradations accurately in CIVA 11 might require significant time and effort.

Manufacturing tolerances: Given that there will be a certain degree of geometric variability, in each flange type, due to manufacturing tolerances, their effect on inspection results should also be further studied. Manufacturing tolerances will affect the ultrasonic beam path of flight through the specimen. This will result in slight variability, with regards to the angle, that the beam will hit a back wall and also the distance it must travel. Although the change in radial

distance should not affect the results to a large degree there could be a significant affect with regards to angle changes. As the red shaded box in figure 2-5 indicates, this region of the flange usually has the widest manufacturing tolerance range. This is also where we propose to place the probe during flange inspections. It is intuitively logical that, as flange sizes increase, the effects of tolerance variability in the red shaded region could have a significant effect on the ultrasonic beams flight of path. A small change in the departure angle of the beam from the probe will result in relatively large changes in the beams target point within a large flange. Comparing simulation results between a flanges with zero tolerance error and results from simulations with a combination of tolerance errors resulting in max geometric distortion is prudent.

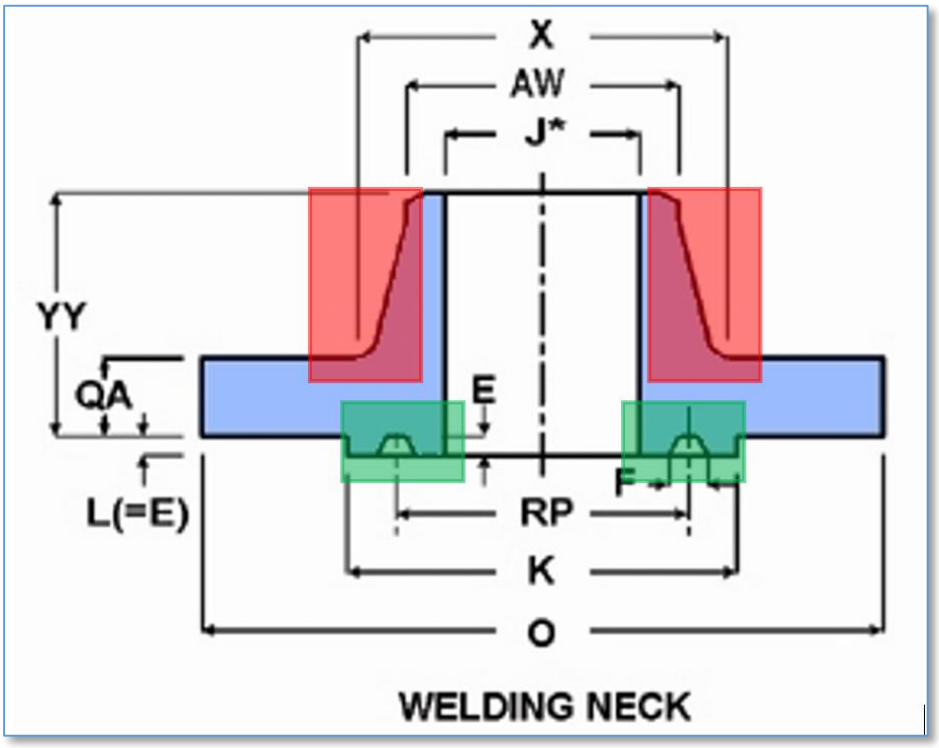

Figure B-3: The figure shows a RTJ welded neck flange. The flange contact surface indicated by the green boxes has narrow manufacturing tolerances. The neck region indicated by the red box, typically where the ultrasonic probe is placed, has a relatively wider tolerance range.

Probe placement: In the context of this paper the inspection procedure for flange inspection relies on a human operator. Since the simulations for this paper assumes that the inspection results are taken from a single point along the flange neck we need to look at how the variability of probe placement during inspection results in variability of the inspection results. If the inspector misplaces the probe a few millimeters up or down from the position that was specified during the simulation, there might be significant differences in results. Further analysis looking at the different simulation results from probe placement variability should also be conducted.

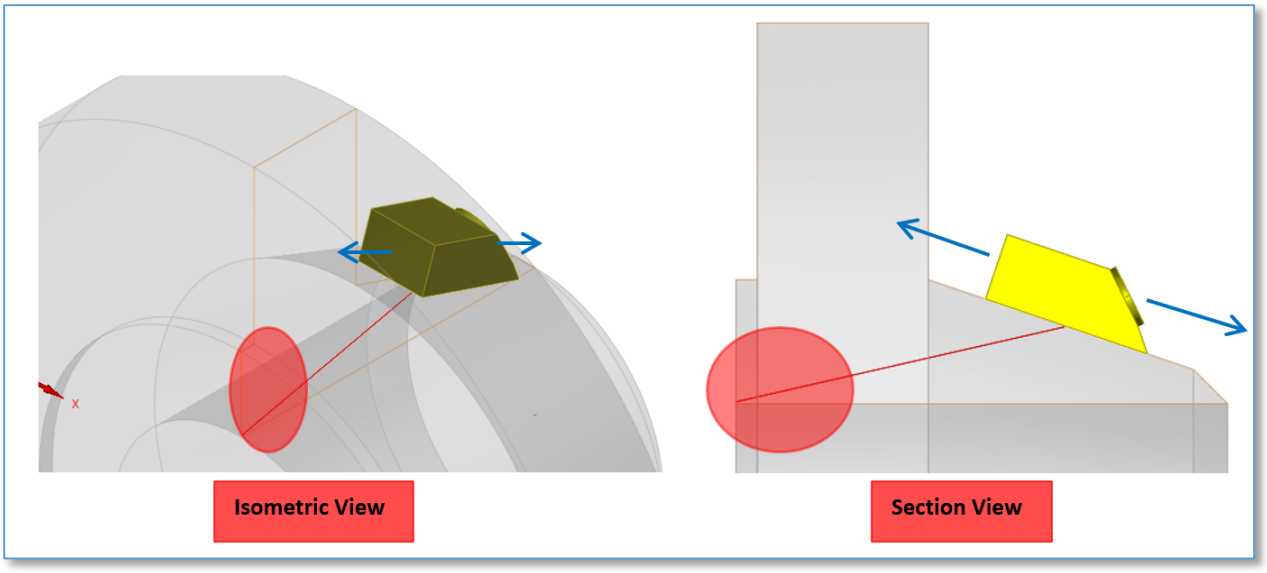

Figure B-4: Red oval indicates region of flaws. Slight misplacement of probe in axis parallel to flow direction could result in beam to back wall and flaw interactions being different from simulation case. Blue arrows indicate placement error axis. Red line indicates ultrasonic beams flight path.

2D vs. 3D modeling: In certain situations one can assume that a 2D cross sectional model can accurately model a 3D object. For example, if one wants to use finite element analysis to predict the hoop stresses in a cylindrical open top water storage tank one does not need to model the tank as a 3D object. One can use the symmetric properties of an object's geometry to simplify the finite element analysis model into an axisymmetric 2D representation. The results of the 2D axisymmetric representation can then be rotated 360 degrees around its rotational axis of symmetry. This assumption holds true when both the model and the load pattern or profile of the model shares the same axisymmetric properties. Hoop stresses arising from hydrostatic pressure within a tank are symmetric along the same rotational axis as the tanks vertical central axis. In the simulated cases in this paper we can assume that the flange is axisymmetric symmetric along a rotational axis parallel to the direction of media flow a 2D representation of the cross sectional plane in line with the central axis of the flange is adequate. If it is assumed that the ultrasonic beam transmitted from the probe into the specimen only follows the incident plane this assumption should hold relatively well, however this assumption must be further verified with inspection results on a real 3D object. As some ultrasonic beam scatter and echoes might not guarantee that the beam will stay within the incident plane there might be a significant effect that is not being considered by the simulation. This is a result of the fact that the ultrasonic beam can be considered as a load in the finite element model but it is obviously not axisymmetric as the model of the flange is. This is due to the fact that the ultrasonic beam, or load, is coming from a point source rather than homogenously spread out in an axisymmetric manner as hydrostatic pressure would be in a cylindrical tank. CIVA UT's Athena 2D finite element analysis module does not allow 3D simulation, as such further studies need to be done along with verification with real inspections on flanges to verify the degree to which the 2D simulation correlates to real world trials (SEGERLIND, 1984).

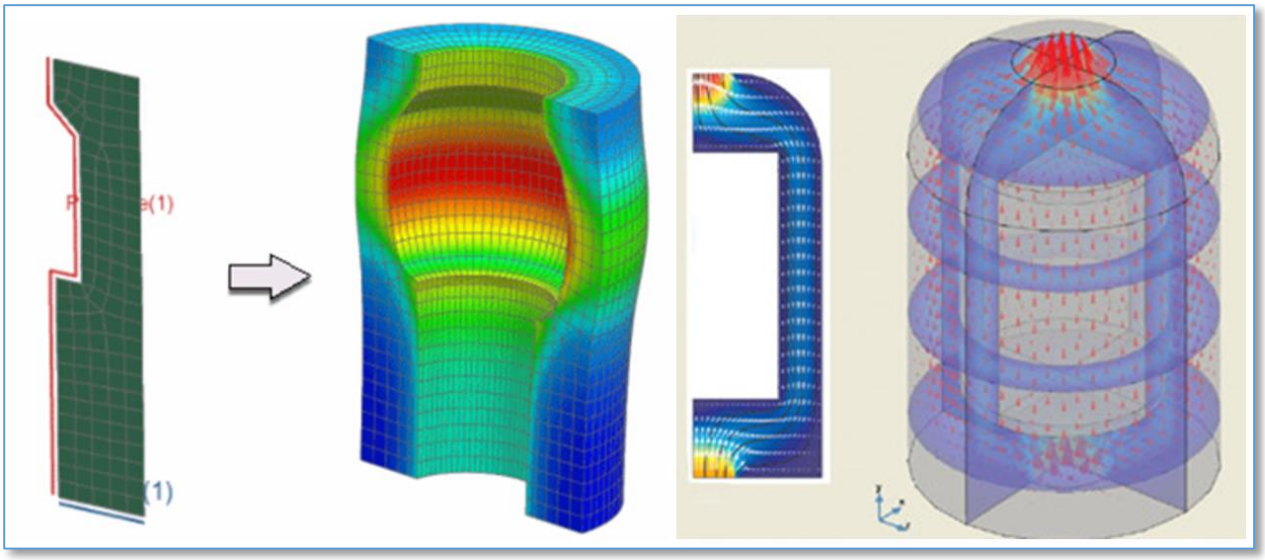

Figure B-5: Some examples of axisymmetric properties to model 3D object as 2D object to reduce computation load.

Appendix C – Semi analytical methods utilized in CIVA UT

Ultrasonic Testing Theoretical Model:

The following section describes the mathematical/scientific models/theories that Civa UT Athena 2D utilizes to perform inspection simulations. This section will focus on the theory behind contact probe modeling and will not describe in detail how submerged probe fields propagate since submerged probe inspection is not a typical inspection procedure of in-service inspection of offshore platform topside static assets. Also, specific phenomenon such as surface roughness and attenuation will not be described as these are user specified rather than fundamental for accurate modeling. The intention is not to give an in depth review of all concepts as this is not the intended scope of this paper, rather it will outline the key theories and models required to adequately simulate natural phenomena in a representative manner which we assume to be in correlated with actual real world experimentation.

Field Computational Model: Civa UT's field computational module serves to calculate the propagation of bulk waves through the specimen being simulated. The ultrasonic field that radiates from the transducer is computed whilst taking into account the coupling to specimen interface depending on the simulation setup. If present and specified the probe wedge and coupling medium will also be taken into account. Information that must be defined for this analysis to be performed;

- Test specimen dimensions and material type
- Transducer (i.e. probe) type, geometric and electroacoustic properties
- Relative position between transducer and specimen
- Points of interest for computation is to take place
- Wave propagation modes between the transducer and the points of interest
- Elastodynamic quantities such as potential and displacement making up the field

Based on the electromagnetic wave theory developed by G.A. Deschamps[5] the electromagnetic waves are transposed to Elastodynamic waves.

Geometric Representation of Beam or "Pencil" Propagation: Civa UT allows the user to predict the propagation of beam through multiple media to verify the interaction of points of interest in test specimen. The pencil model predicts bulk wave propagation from the transducer point source by predicting various elastodynamic quantities corresponding to ultrasonic energy paths. Ultrasonic energy paths differ with respect to transmission through or refection from interfaces and whether or not the wave undergoes mode conversions.

[5] G. A. Deschamps, « Ray techniques in electromagnetics », Proc. I.E.E.E. 60 (1972), pp.1022-1035.

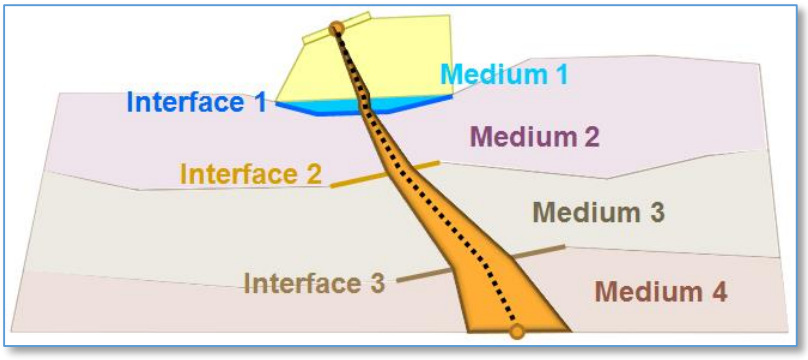

Figure C-1: Note how the "pencil" of rays propagates and refracts with or without backwall reflection. Propagation starts at source point (i.e. the transducer). Depending on the nature of mediums and whether or not backwalls have caused reflection there could be several energy paths or sections. Different energy paths correlate to changes in direction and spread of field. These are accounted for geometrically by the simulation software.

For an axial ray a pencil can be defined as a mathematical object. For a given wave propagation mode starting at the source point the pencil follows a specified geometric path of energy to a given point of interest.

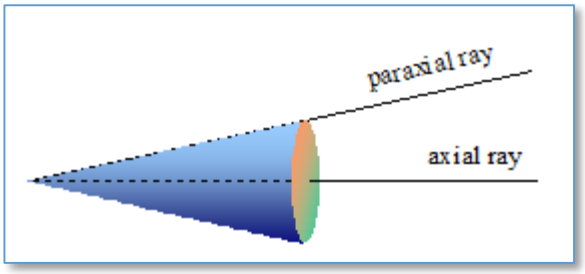

Figure C-2: Pencil represented as a conical path defined by the paraxial ray and the axial ray. The point source on the left originates from the transducer.

Defining a Pencil with Differential Parameters:

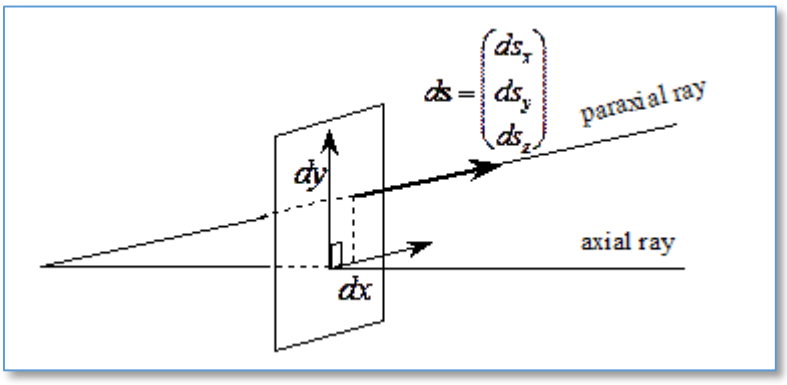

Figure C-3: Pencil represented as constituent differential parameters

A vector *dx* is defined as the paraxial ray's deviation given a specific time propagation. Given the reference frame defined by *z*, *xy*, and the axial ray direction. Coordinates *dx* and *dy* are perpendicular to *z*. Velocity of deviation for the paraxial ray relative to the axial ray is infinitesimal in nature and is identified by *ds*, the slowness vector. Two of the three components are independent. The third component must be determined by the first two components, type of wave, and the local properties of the medium which the wave travels. The quadrivector {*dx*, *dy*, *dsx*, *dsy*} describes the pencil relative to the axial ray at any given instance in time (GENGEMBRE and LHEMERY, 2000).